

# What Are You Doing? A Closer Look at Controllable Human Video Generation

Emanuele Bugliarello<sup>1</sup>, Anurag Arnab<sup>1</sup>, Roni Paiss<sup>1</sup>, Pieter-Jan Kindermans<sup>1</sup> and Cordelia Schmid<sup>1</sup>

<sup>1</sup>Google DeepMind

High-quality benchmarks are crucial for driving progress in machine learning research. However, despite the growing interest in video generation, there is no comprehensive dataset to evaluate human generation. Humans can perform a wide variety of actions and interactions, but existing datasets, like TikTok and TED-Talks, lack the diversity and complexity to fully capture the capabilities of video generation models. We close this gap by introducing ‘What Are You Doing?’ (WYD): a new benchmark for fine-grained evaluation of controllable image-to-video generation of humans. WYD consists of 1,544 captioned videos that have been meticulously collected and annotated with 56 fine-grained categories. These allow us to systematically measure performance across 9 aspects of human generation, including actions, interactions and motion. We also propose and validate automatic metrics that leverage our annotations and better capture human evaluations. Equipped with our dataset and metrics, we perform in-depth analyses of seven state-of-the-art models in controllable image-to-video generation, showing how WYD provides novel insights about the capabilities of these models. We release our data and code to drive forward progress in human video generation modeling at <https://github.com/google-deepmind/wyd-benchmark>.



Figure 1 | Samples from our WYD dataset (above) and from the commonly used datasets for controllable human video generation (below). WYD contains significantly more diverse videos, in terms of number of actors, actions, interactions, scenes as well as camera motion.

## 1. Introduction

Video generation has witnessed tremendous progress driven by recent advances in generative modeling [78, 33, 80, 31, 51, 19, 8]. The field spans a wide range of tasks, such as text-based generation [72, 34, 2, 46], image animation [36, 60, 6, 94] and stylization [25, 18, 14, 73]. In this paper, we focus on controllable human video generation. Controllable generation enables artists to precisely specify *how* a generative model creates content, by conditioning models spatially (e.g., bounding boxes, masks, poses, depth and edge maps) [40, 57, 87, 64] and temporally (e.g., motion vectors and camera positions) [27, 70, 99]. In particular, controllability is crucial for human generation, given the complexity of precisely describing human movements in words and its practical applications (e.g., simulating a risky stunt in a movie, or making someone else follow a dance).

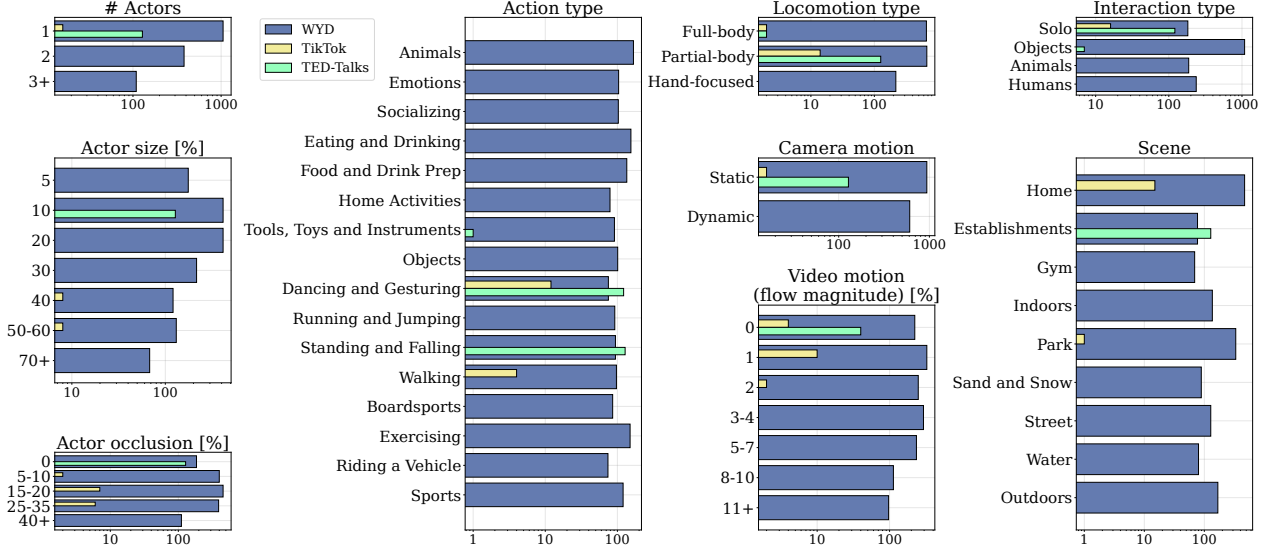


Figure 2 | **Diversity of wYD.** wYD contains manually-labeled fine-grained annotations for 9 categories and 56 sub-categories relevant to human video generation. Manually annotating TikTok and TED-Talks, we observe their distinct lack of diversity across all nine categories.

As the popularity of this field has grown, the gap between model capabilities and their evaluations has, however, widened. Image generation benefits from detailed evaluation protocols [90, 41, 37] but video evaluation is still in its early stages. Specifically, evaluating controllable human video generation has received limited attention. Humans are one of the most important real-world entities, perform a wide variety of actions, interact with animate and inanimate objects through complex dynamics, and display a range of emotions. The community typically relies on two datasets: TikTok [39] and TED-Talks [71], which have limited size (Tab. 1) and a *narrow scope*, such as a single person dancing or talking in a static shot (Figs. 1 and 2). These make them insufficient to reveal the full potential and shortcomings of existing models.

We argue that a detailed evaluation of models’ capabilities across fine-grained categories is needed to pinpoint development areas and compare different models, but this level of detail is missing from current benchmarks [74, 95, 65]. To bridge the gap between model capabilities in generating human videos and what evaluations can capture, we introduce ‘What Are You Doing?’ (wYD): a new dataset of complex, dynamic videos with a wide variety of human appearance, actions and interactions. wYD includes diverse and high-quality videos filtered semi-automatically, and rigorously finalized by detailed manual verification (400+ hours). In particular, we built wYD considering the typical setup of controllable image-to-video generation (*e.g.*, animating a person with specific movements) [12, 53, 69, 104, 3, 60, 42, 83, 86, 96, 44] by ensuring human actors are clearly visible in the first frame. Notably, while prior benchmarks are limited to dataset-level evaluations, we label the 1,544 samples in wYD according to nine categories and 56 sub-categories, enabling systematic evaluations of key aspects of video-level and human-level generation. Overall, wYD is significantly larger and broader than existing benchmarks for controllable human video generation (see Tab. 1 and Fig. 2).

To reliably measure the performance of controllable video generation models at synthesizing humans, we propose an evaluation protocol that spans key aspects of video generation (*i.e.*, video quality, per-frame correctness, and video motion) as well as human-centric ones, enabled by further annotating the *human actors* in wYD with manually-verified video segmentation masks. We perform extensive human studies of automatic metrics, and select those with best alignment. In doing so, we find that our pose-based metric (pAPE) better quantifies the fidelity of generated human movements.

	TikTok	TED-Talks	wyD
# Videos (unique clips)	16 (14)	128 (40)	1,544 (1,393)
Video duration [s]	8.3–23.0	4.3–23.1	1.5–15.0
Video aspect ratio	portrait	landscape	portrait and landscape
# Actors	1	1	1, 2, 3+
# Words [avg (std)]	N/A	N/A	21 (12)
			# actors, actor size
Categories	N/A	N/A	% occlusion, actions, scene interactions, locomotion camera and video motion
Additional annotations	dense poses	N/A	video segmentation masks

Table 1 | **Overview of data statistics.** wyD complements existing datasets for human video generation with more videos, higher diversity and fine-grained categories. See Fig. 2 for more statistics.

As a representative use case of our benchmark and evaluation protocol, we investigate seven families (and ten variants) of controllable video generation models, which include commonly used pose, depth and edge conditioning signals [96, 13, 107, 62, 17, 49, 85]. Our results from both human and automatic evaluations show that, using wyD, we can diagnose several limitations of current SOTA models, facilitated by the diverse and fine-grained categories unique to our dataset. These include challenges that cannot be measured with existing datasets, such as generating cross-shot or atypical movements, interactions with objects, and more.

In summary, our contributions are fourfold. (i) We identify the limitations of existing benchmarks for controllable human animation, and meticulously collect wyD: a large and highly diverse benchmark with fine-grained annotations. (ii) We propose a standardized evaluation protocol with metrics that have been validated with human preferences. (iii) These include new and adapted people-centric metrics, such as pAPE: a new metric to quantify the adherence of generated videos to human movements from detected poses. (iv) We conduct system-level evaluations of ten SOTA models on wyD, and show that it is harder than existing benchmarks, revealing six systematic limitations and narrow training data distributions that were previously undetectable.

## 2. Related work

**Controllable video generation.** Video generation is a challenging task, with significant strides made in recent years [80, 46, 2, 6?, 32, 33, 31]. While text is the main modality to steer video generation models, there is a growing trend towards using detailed visual signals for finer control. Examples include depth maps [17, 93, 102, 106], human poses [35, 83, 92, 96], optical flow [70, 84, 89, 101], bounding boxes [15, 82] and camera angles [27, 89], among others [26, 49, 99]. In this work, we focus on poses (common for controllable human generation) as well as depth and edge control signals (generally used for dense conditioning).

**Benchmarks for video generation.** Prior work typically evaluates video generation models on datasets originally created for discriminative video recognition tasks [9, 65, 74]. More recently, a few datasets have been proposed for video generation, typically of text prompts for the text-to-video task [38, 54, 64]. I2V-Bench [68] assesses image-to-video consistency, while StoryBench [7] evaluates video generations from a sequence of text prompts. Unlike wyD, these datasets do not enable fine-grained studies of (controllable) human generation (e.g., actions, interactions, and sizes).

**Benchmarks for human video generation.** Models for human animation often evaluate performance on two datasets, TikTok [39] and TED-Talks [71, 83]. The TikTok dataset consists of just 16 videos scraped from TikTok, where there is only a single person at home, who covers a large, centered

part of the video and mostly dances in place. The TED-Talks dataset contains 128 videos from 40 talks at TED, where a single person is on stage and gesticulates while speaking on their spot. In this paper, we present WYD as a solution to their shortcomings for controllable human video generation. Compared to TikTok and TED-Talks, it is orders of magnitude larger and much more diverse (Fig. 2), and it is not limited to single-person close-up videos.

**Metrics for human video generation.** Previous work evaluates models using pixel-level metrics, like SSIM and LPIPS, and FID [30, 88, 105]. With human studies, we show that the ubiquitous FID is inaccurate as it lacks temporal consistency, and FVD [79] is preferred (which cannot be computed reliably in small datasets like TikTok and TED-Talks). We also introduce metrics to quantify the quality of generated *people*.

### 3. The What Are You Doing? (WYD) benchmark

Our goal is to measure the performance of video generative technologies at synthesizing humans in real-world settings. We are primarily interested in human animation, given its practical applications and popularity in the field. To effectively do so, a benchmark that satisfies different desiderata is required. Specifically, we need videos with (i) high-quality descriptions, and wherein people (ii) are visible, (iii) perform a variety of actions, (iv) interact with each other and other objects, within (v) natural contexts of complex and dynamic everyday scenes. In this section, we describe our approach to curate videos that meet these criteria from previously published datasets, and how we categorize them in order to assess different aspects typical of human video generation.

We refer to our new dataset as *What Are You Doing?* (WYD) as video generation models are tasked to generate videos of high-quality humans across very diverse settings.

#### 3.1. Data filtering

To construct a *generic* benchmark for human video generation, we require videos that capture a wide range of human activities and environments. Therefore, we rely on three publicly licensed datasets collected from Internet platforms, such as YouTube and Flickr: Kinetics [43], DiDeMo [29] and Oops [22]. These datasets include humans with different body poses, clothing, age and background, and performing a great variety of actions (including unintentional actions that serve as an interesting testbed for atypical human modeling).

High-quality text descriptions are necessary to accurately evaluate text-guided video models. For the datasets above, StoryBench [7] includes human-written captions for video generation, as well as useful metadata, including event boundaries and actor identification (*i.e.*, the entities with a key role) in a video [81]. WYD leverages StoryBench annotations, but we treat each video segment separately (rather than as part of a sequence) in our 7-step pipeline (see Appendix B for examples of discarded and retained videos at each step).

**1. Videos with human actors.** We start by filtering out videos where the main actors are not humans. For Kinetics and Oops videos, we use human-labeled metadata in StoryBench, which associates each caption to its main actor (*e.g.*, “man with white t-shirt”). For DiDeMo, we extract the main actors of each caption with an instruction-tuned LLM [24] (note that it is not trivial to use object detectors to extract the main actors due to non-salient humans in a video). From 600+ actors, we manually identify 224 referring to humans.

**2. Removing scene cuts.** Most of the original videos are single shot, but we found a few of them with multiple scenes. We use a shot detector [11] and whenever it detects 2–4 cuts, we remove the video if none of the parts lasts for at least 80% of the original duration. Otherwise we replace the original video with that part. Doing so allows us to remove scene cuts while preserving the actions described in the captions.



**3. Ensuring visible humans.** People performing the main action in the video need to be visible, especially in the first frame, to evaluate how image-to-video systems can generate them. We annotate our videos with a state-of-the-art human pose estimator [100], and keep only those in which people are ‘mostly visible’ (defined as 11/18 body keypoints detected) in the first, and at least 70% of the frames.

**4. Removing short and long videos.** Given that our primary goal is to evaluate human video generation, we take into account the capabilities and the computational resources of most existing models to date, and opt to limit videos in our benchmark to a duration between 1.5s and 15s.

**5. High text alignment.** The captions for Kinetics and Oops videos were originally made from the perspective of a specific actor [81]. As a result, some captions fail to naturally describe the most salient actors in a video. To minimize such cases, we only keep the actor whose video–caption pairs have the highest similarity according to a fine-grained contrastive VLM [23]. With the same approach, we then remove the bottom 25% of the videos to maximize text controllability.

**6. Minimum resolution.** We further filter down our data to only include videos with smaller edge of at least 360 pixels, to ensure references of higher quality while keeping enough samples for statistical significance.

**7. Manual verification.** Finally, we meticulously scrutinize the quality of the resulting videos and remove those with (i) significant blur, (ii) poor lighting, (iii) unstable camera, (iv) low motion, (v) unclear captions, or (vi) where the first frame does not capture the main actors. This process, in conjunction with the video categorization below, was done in multiple rounds and took over 250 hours of annotation time. The authors validated the annotations and sought to ensure that the videos had high diversity and would be challenging for current video generation models.

At the end of this pipeline, WYD contains 1,544 high-quality videos (from the original 18,351) which enable the fine-grained analyses described next at a tractable runtime.

### 3.2. Video categorization

A key goal of our benchmark is to enable fine-grained understanding of the capabilities of video generation models to synthesize humans across different facets; rather than reporting a single aggregated score, as done with other datasets. To achieve this, we annotate our data with nine categories that capture important aspects for synthesizing videos of humans. Each category in turn contains sub-categories (see Fig. 2 for an overview), each with at least  $\approx 100$  samples so as to provide sufficient statistical power for our analyses.

**Number of human actors.** For each video in WYD, we manually label the exact number of humans performing the main actions (*i.e.*, salient for generation), and then group them in three groups (1, 2, 3+). Notably, each sub-category presents specific challenges, from consistently generating multiple people to more dynamic videos with a single person.

**Human actor size.** The size of human actors can affect how well a video generation model performs. We manually estimate the area covered by the human actors in each video, and categorize them into seven splits of actor size (Fig. 2).

**Human occlusion.** Object consistency is crucial in generated videos, and humans need to keep their appearance despite partial or full occlusions. We measure the average number of body keypoints detected by the pose estimator [100], and categorize our videos into five ranges of human actor occlusion (*i.e.*, percentage of keypoints that are not visible).

**Human actions.** The ability to perform a wide range of actions is a distinctive characteristic of humans, and different actions may require disparate generation capabilities (e.g., swimming vs. eating). We manually assign action labels to each video in multiple rounds, adjusting the levels of specificity after each round. This process yields sixteen sub-categories of visually similar actions (as shown in Fig. 2).

**Human locomotion.** We manually classify human body movements into three categories: full-body, partial-body, and hand-focused. While full-body motion indicates actors changing location in the video, partial-body motion involves only moving part of the body (e.g., the arms). We label videos where hands’ motion is crucial separately, as existing models often struggle to generate hands [103, 55, 47].

**Camera motion.** We manually label each video as dynamic if the camera follows the actor, or static otherwise.

**Video motion.** The primary aspect that differentiates videos from images is the motion within them. We use an optical flow model [76] to estimate the amount of motion in each video, which we then use to study how this key aspect affects human video generation across seven motion ranges.

**Actor interactions.** Humans often interact with their environment, either through inanimate objects, animals or other humans. Object interactions are often hard to generate, as they require a deeper understanding of shapes, texture and the physical laws of the world. While previous work only evaluates solo actions [39, 71, 12], our annotations show that most of the videos in our dataset involve interactions.

**Scene.** Different actions are associated with different environments (e.g., swimming) and video generation models should be able to synthesize a variety of environments. We manually annotate the videos in WYD with nine different scenes where actions take place (both indoors and outdoors).

**Discussion.** We find that only a few categories overlap with each other significantly (see Fig. 40 in Appendix B). Namely, actions and interactions with animals; and video and camera motion, where high-motion videos come from dynamic camera, and videos with low motion correspond to static camera. Interestingly, high-motion videos do not necessarily involve fewer people, but small people are often associated with high motion and full-body movement of a single actor.

### 3.3. Video segmentation masks

In addition to labeling our videos with 56 sub-categories, we also annotate each human actor in a video with tracked segmentation masks. To do this, we first identify people in the first frame of each video via bounding boxes using OWLv2 [59]. After selecting and refining the bounding boxes corresponding to the actors only, we feed them as input to SAM 2 [67], which returns video segmentation tracks for each of the actors. These tracks are further verified and manually corrected at the frame level by the authors, an effort that took over 150 hours (see Appendix B). We use them to define new automatic metrics for WYD by analyzing model performance at the human level, as discussed next.

## 4. Evaluation protocol

We propose the following evaluation metrics (extensively validated in Sec. 6) to evaluate model performance on WYD across three aspects: video quality, frame-wise similarity, and motion similarity. While previous work only evaluates the entire videos, we also propose human-level metrics here.

### 4.1. Video-level evaluations

To measure performance for the entire generated videos, we use the following existing metrics (more details in Appendix D).

**Video quality.** Following prior work [68, 87], we use FVD [79] with an I3D [10] model for overall video quality.

**Frame-by-frame similarity.** In addition to being smooth and appealing, videos generated by controllable models need to abide to their references. We measure frame-wise visual similarity using the features extracted by a DINOv2 [61] encoder, which was used in previous work for similar tasks [75]. To align with other metrics, in the following, we report the complement of the similarity between reference and generated features, and denote it as ICD (image cosine distance).

**Video motion.** Following prior work [49, 54], we compute the optical flow endpoint error (OFE) as a measure of structural dissimilarity between reference and generated videos. We use RAFT [76] to compute the optical flows.

## 4.2. Human-level evaluations

As humans are the main focus of WYD, we propose the following metrics to measure performance at the human level, by leveraging our collected segmentation masks.

**Video quality.** We re-use FVD but set to black any pixels outside the collected segmentation masks corresponding to the human actors in a video, which we refer to as pFVD.

**Frame-by-frame similarity.** At the human level, we average the DINOv2 features of the patches corresponding to the segmentation masks of all the actors in a video (pICD).

**Human movement.** The equivalent of video motion for humans should measure how closely synthesized people align with their counterparts in the reference video. To do so, we propose a *new metric* that computes the average precision (AP) between the 2D poses detected in the reference and generated videos. We extract the poses using the state-of-the-art DWPose [100], and compute AP using pose key-points similarity as a similarity metric. In practice, we identify human actors by matching the bounding boxes of detected people in a generated video with those from the reference segmentation masks using the Hungarian algorithm, and only compute AP against the poses of those *actors*. We measure AP for each video separately for better interpretability, and report the complement of the average AP (*i.e.*,  $1 - \text{AP}$ ) as a metric, which we call pAPE (pose average precision error).

## 5. Results on controllable video generation

We use our new WYD dataset to investigate, for the first time, how difficult different facets of human generations are for state-of-the-art controllable video generation models (as a representative use case of models capable to do precise human generation). We show that WYD allows us to pinpoint six novel failures in ten existing models. To facilitate this, we open-source the data as well as the code to fully reproduce our evaluations and results, which required significant computational resources (over 5,000 A100 GPU hours). Our evaluations are at 16fps, and refer to this version as WYD<sub>16</sub>.

In this section, we overlay our results by referring to specific failures of video generation models. As samples require significant space, we report them in Appendix A for reference.

**Experimental setup.** We focus on state-of-the-art (SOTA) image-to-video models with pose, depth or edges conditions. To fairly evaluate these models, we perform system-level evaluations and adopt their original pre-processing pipelines.

Pose key-points are the most common way to condition generative models to synthesize humans. They are relatively sparse, and allow artists to quickly generate humans in specific poses without having to match specific body measures. We look at four recent, open-source SOTA models: MagicAnimate [96], MagicPose [13], MimicMotion [107] and ControlNeXt-SVD-v2 [62] (henceforth, ControlNeXt).

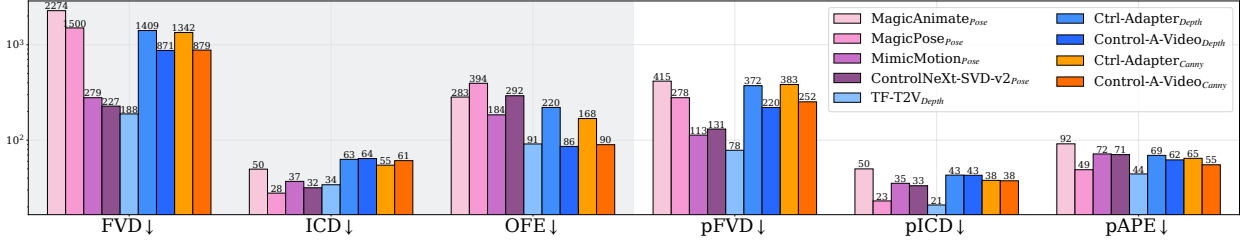


Figure 3 | Overall performance (left: video-level, right: human-level) of SOTA controllable image-to-video models on  $WYD_{16}$ . Pose models are shown in pink, depth ones in blue, and edge ones in orange. Human generation is multifaceted and no model prevails across all metrics.

Depth and edge maps are the typical conditions for dense, pixel-level guidance of generative models. We analyze three open-source, SOTA models that can be guided with text, depth or edges: Control-A-Video [17], Ctrl-Adapter [49] and TF-T2V [85]. Notably, the first two models can only generate a few frames, and we extend their generations auto-regressively to match the duration of the reference videos.

We note that these models have been trained on internal datasets (or private subsets of public data) which did not include any  $WYD$  videos, as confirmed by the authors (Appendix A). In particular, pose-based models have mostly been trained on close-up single-person videos. While they may incur a distribution shift on  $WYD$ , we believe controllable human generation should go beyond those simple cases, and we propose  $WYD$  as a more general and challenging benchmark.

**Overall performance on  $WYD_{16}$ .** Fig. 3 shows the overall performance of pose-, depth- and edge-conditioned models on our new  $WYD_{16}$ . We find that the recent MimicMotion and ControlNeXt overall outperform other pose-guided models, while depth-conditioned TF-T2V is the best in general. Looking at pose-guided models, MagicAnimate is often the worst model, and we found it to generate extremely distorted humans, which we attributed to its dense pose detector (Appendix A). Due to its flickering, MagicPose obtains poor *video quality* (FVD, pFVD) but results in better *humans* (pICD, pAPE) than MimicMotion and ControlNeXt, as well as *frame similarity*, as the model was trained to preserve the identity and background information, yielding lower ICD.

Looking at depth- and edge-guided models, we see that Control-A-Video and Ctrl-Adapter perform rather poorly. Inspecting Control-A-Video’s generations, we observe that they follow the underlying signal well but at the expenses of distorted colors and artifacts. Ctrl-Adapter’s performance vastly improves when adding text to the guiding signals (as shown in Appendix C), albeit with videos drastically degrading after one second (the training duration of the model).

**$WYD$  is harder than previous benchmarks.** In Fig. 4, we compare the errors in human metrics between  $WYD$  and TikTok or TED-Talks. We find that  $WYD$  is consistently harder in both visual quality and movement, with error rates 1.8–4.6× higher for pICD, and 1.8–12.3× higher for pAPE.\* That is,  $WYD$  poses significant challenges to SOTA systems, suggesting that it can be used to drive progress in this area.

### 5.1. Diagnosing model performance

We use our video categories and automatic metrics to identify and study the limitations of the best performing models on  $WYD$  (MimicMotion, ControlNeXt and TF-T2V).

**Identities collapse.** When looking at videos with 3+ *actors*, we discover that models blend their appearances, especially when *humans interact* with each other (see Appendix A). TF-T2V better

\*NB: FVD is unreliable in small datasets like TikTok and TED-Talks.



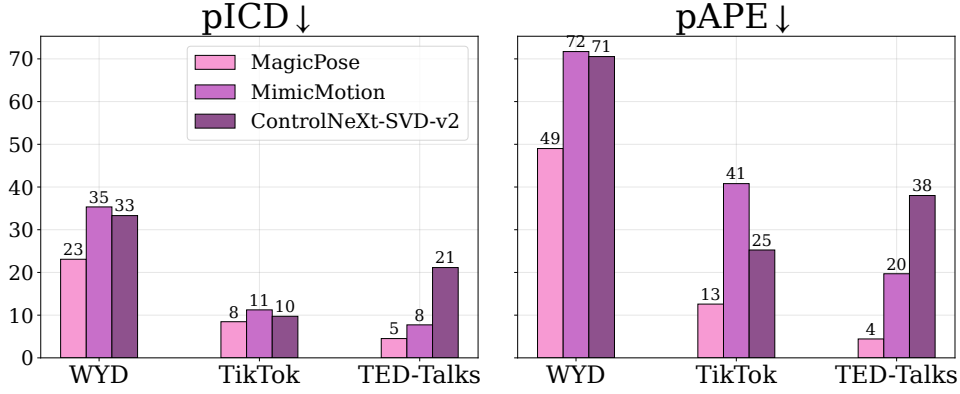


Figure 4 | Performance comparison between WYD, TikTok and TED-Talks for pose-conditioned models. WYD yields larger errors, confirming that its greater diversity is more challenging for models.

preserves human identities than other models, but it struggles more with facial traits, as reflected when evaluating it on *large humans* (70% size) and shown in Fig. 5.

**Vanishing objects.** Shockingly, pose-guided models tend to discard *animals* and objects they interact with, resulting in surreal generations like people floating in the air (Fig. 6).

**Atypical motion is always hard.** In addition to fast and complex motion (e.g., Fig. 7), we see that even slow, atypical movements with static cameras are hard to generate, such as a person getting up using their arms.

**Smaller is harder.** The variety in human sizes in WYD lets us find that current models fall short in generating videos of *small humans*. Typical failures include changing a person’s appearance, producing unnatural motion, or even removing them entirely (as shown in Appendix A for example).

**Large displacements are hard.** Surprisingly, current models, and especially pose-guided ones, struggle to generate realistic movements when humans cross the shot or the camera follows them. These videos often occur *outdoors* and include actions such as *boardsports* or *running and jumping*, have *full-body* locomotion and/or *high video motion*. Similarly, models fail to perform *quick* actions (e.g., backflipping), often leading to static videos in pose models. That said, there is a smaller performance gap between *static and dynamic camera motions* for TF-T2V, as depth maps capture background information useful for camera motion.

**Occlusions are challenging.** Finally, our dataset and metrics let us verify and quantify the expected challenges in generating humans under higher levels of *occlusion* (Appendix A).

**Beyond WYD categories.** WYD captures a variety of real-life situations, which allow us to uncover a few more failure modes beyond our annotated categories; such as the lack of commonsense in pose-guided models (interacting with objects does not change their state), or tendencies to steer humans towards narrow age groups and beauty ideals (Appendix A).

## 6. Validating automatic metrics

Automatic evaluation metrics are instrumental in benchmarking a model’s performance. However, automatically evaluating different aspects of video generation is difficult: While multiple metrics have been proposed [90, 91, 28, 97], many have been shown to have little correlation with human preferences [7, 45, 50, 63, 64]. Therefore, a careful validation of the metrics is a crucial aspect for a trustworthy protocol.

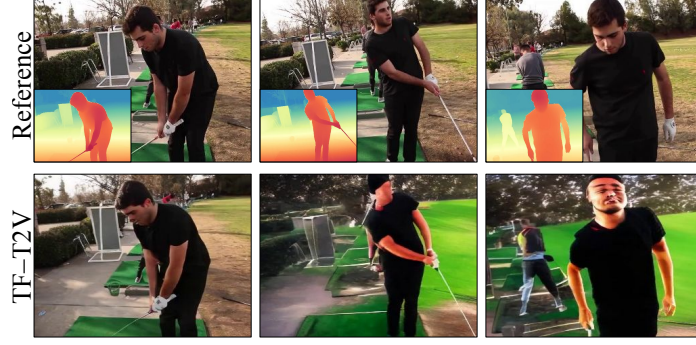


Figure 5 | Example of SOTA depth-conditioned TF-T2V model failing to preserve people’s identities.

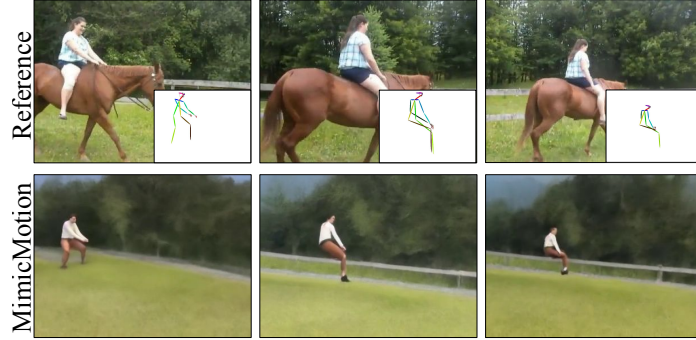


Figure 6 | Example of SOTA pose-conditioned MimicMotion model making animals vanish.



Figure 7 | Example of SOTA pose-conditioned MimicMotion model struggling to generate humans performing fast and complex motion.

In this section, we validate our proposed evaluation framework (Sec. 4). We compare our selected metrics with alternatives for each of the key generation aspects defined in Sec. 4 (visual quality, frame similarity, and motion), showing that our metrics reflect human preferences (see Tab. 2).

**Validation setup.** We assess the performance of different metrics by aligning them with human judgments in two settings. First, we perform side-by-side model comparisons. We use four templates to assess video quality, frame-wise fidelity, video motion and people movements. Second, we extensively verify the model rankings given by the metrics with generated samples. We refer to Appendix D for more details.

**FVD better measures video quality.** We compare different metrics as proxies for overall video quality: FID, FVD, JEDI [97] (a recent distributional video metric) and VMAF [48] (Netflix’s perceptual video quality metric). We report Spearman rank correlation between ranked human judgments from all 21 model pairs and the scores of each metric in Tab. 2, which shows how FVD and JEDI much

	Metric	Performance [%]
Video quality	FVD	<b>96.36</b>
	FID	22.24
	JEDi	<b>96.36</b>
	VMAF	29.65
Video motion	OFE	<b>82.10</b>
	DPT	67.37
Human quality	ICD	<b>72.67</b>
	PSNR	59.04
	RMSE	38.55
	SSIM	62.65
Human movement	pAPE	<b>71.95</b>
	pOFE	61.45

Table 2 | **Side-by-side evaluations.** We report Spearman rank correlation for video quality, and pair-wise accuracy for the rest. Our selected metrics agree with human preferences from SxS studies.

better agree with humans. Importantly, Fig. 8 shows that the widely used FID metric (*e.g.*, to compare generations on TikTok and TED-Talks) is inadequate, favoring MagicPose videos due to their sharpness, despite their inconsistencies due to significant flickering. Appendix A also shows that Control-A-Video’s samples are characterized by highly distorted colors due to auto-regressive generation, but VMAF ranks it first (Appendix D). We opt for FVD as it is much faster and it is also reliable at the human level (shown in Appendix D), and advise against using FID to measure video quality.

**ICD captures frame-wise quality.** We evaluate the ability of visually-controlled models to produce content similar to their references by following the conditioning signals. For this, we compare our DINO-based ICD metric (Sec. 4) with pixel-level ones, such as RMSE, PSNR and SSIM. In Appendix D, we show that PSNR, RMSE and SSIM favor the generations by MagicAnimate over those by Ctrl-Adapter even though the qualitative samples reveal the opposite. This behavior is likely caused by pixel-level metrics rewarding MagicAnimate to retain the background well. On the other hand, ICD agrees with human preferences more, as shown by a 10% increase in accuracy over other metrics in Tab. 2.

**OFE for overall video motion.** For structural similarity between generated and reference videos, we compare the optical flow endpoint error (OFE) against the similarity between extracted depth maps, measured by the standard  $\delta_1$  metric [21] (DPT) with Depth Anything v2 [98]. On WYD, DPT assigns a higher score to Ctrl-Adapter than to Control-A-Video, although we find that Control-A-Video follows the control signals more accurately than Ctrl-Adapter (at the expenses of visual quality). Therefore, we opt for OFE to measure video motion, which also achieves 15% higher pair-wise ranking accuracy in side-by-side evaluations (Tab. 2).

**Measuring human movement via detected poses.** We introduce pAPE, a new metric that measures the complement to the AP of pose key-points between reference and generations. Tab. 2 shows that pAPE agrees 10% more often than human-level OFE (pOFE) on human evaluations of people’s movements. As shown in Fig. 9, MimicMotion and ControlNeXt do not achieve good pAPE despite high visual quality (FVD). Analyzing further, we find that they always re-scale and re-center the generated humans (see Fig. 10). We discover that this behavior is part of the models’ pre-processing code [77, 20], and might stem from the overdependence on simpler datasets, with only a single, large, centered actor. This further emphasizes the need for more diverse benchmarks for controllable human video generation, like WYD.

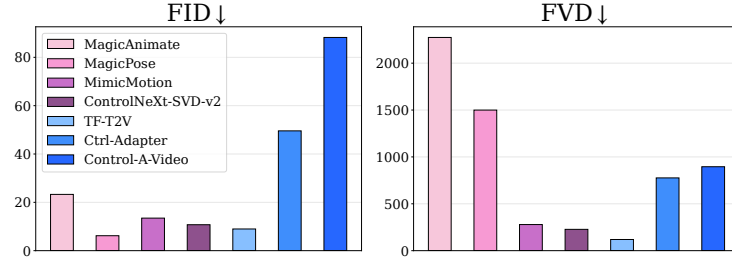


Figure 8 | Comparison of video quality metrics on WYD. Unlike FID, FVD penalizes generations with flickering and artifacts.

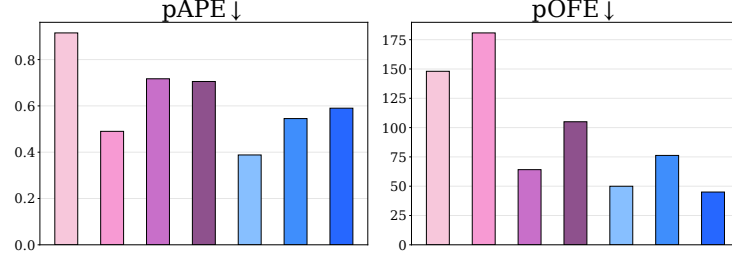


Figure 9 | Comparison of video quality metrics on WYD. pAPE correctly finds issues with MimicMotion and ControlNeXt (Fig. 10).



Figure 10 | Example of pose re-scaling in MimicMotion. The pose detected in the generated video (bottom right) is re-scaled and re-centered compared to the pose from the reference video (top right). Humans are not sensitive to such changes but our pAPE metric is.

**Limitations of our metrics.** While our metrics show better accuracy with human preferences, we point out a few of their current limitations. Firstly, the pose estimator used in *pAPE* detects humans in each frame independently, resulting sometimes in incoherent sequences, as well as incorrect or hallucinated poses from poorly generated people. Secondly, our *video quality metric* suggests that it is easy to generate videos with object interactions. However, looking at pose-conditioned models, we find that objects often disappear. As they cover a small percentage of the frame, metrics like FVD are not largely affected by this, and fail to show this problem.

We do not investigate metrics for face quality, but notice that faces are often of poor quality. This makes it challenging to evaluate *emotions*, especially when humans are small.

Finally, our evaluation protocol is based on visually-conditioned image-to-video models. This allows us to propose metrics like pICD and pAPE that better measure human-level properties via segmentation masks. We encourage future work to propose metrics for text-only video generation.



## 7. Conclusion

Video generation has a tremendous potential to impact our society, and it is thus imperative to comprehensively assess model capabilities. As a milestone to this end, we collected `wyD`: a dataset to evaluate the synthesis of humans in real-world settings. Our analysis showed that `wyD` is more diverse and challenging than prior benchmarks for controllable human video generation. It is equipped with fine-grained categories that allowed us to discover several failure modes of state-of-the-art technologies, through both automatic and human evaluations. By releasing `wyD`, we aim to move beyond the current narrow scope of close-up single-person human video generation, and to drive forward progress towards the more ambitious goal of *generic* human generation.

We focused on visually-conditioned image-to-video generation technologies in this work, as methods capable of precisely controlling human actors. A promising direction for future work in evaluating human video generation technologies would be to develop vision tools to assess performance of text-to-video models, by taking inspiration from current work in text-to-image generation [37] and tackling the challenges posed by the time dimension in videos.

## Acknowledgments

We would like to thank Thomas Mensink, Jordi Pont-Tuset, Benoit Corda, Monika Wysoczańska, Thomas Kipf, Nikos Kolotouros, Paul Voigtlaender, David Ross, Miki Rubinstein, Tomáš Izo, Rahul Sukthankar, and the Veo team for fruitful discussions and support throughout this project.

## References

- [1] Bain, M., Nagrani, A., Varol, G., Zisserman, A.: Frozen in Time: A joint video and image encoder for end-to-end retrieval. In: ICCV (2021)
- [2] Bar-Tal, O., Chefer, H., Tov, O., Herrmann, C., Paiss, R., Zada, S., Ephrat, A., Hur, J., Liu, G., Raj, A., Li, Y., Rubinstein, M., Michaeli, T., Wang, O., Sun, D., Dekel, T., Mosseri, I.: Lumiere: A space-time diffusion model for video generation. In: ICML (2024)
- [3] Bhunia, A.K., Khan, S., Cholakkal, H., Anwer, R.M., Laaksonen, J., Shah, M., Khan, F.S.: Person image synthesis via denoising diffusion model. In: CVPR (2023)
- [4] Birhane, A., Prabhu, V.U.: Large image datasets: A pyrrhic win for computer vision? In: WACV (2021)
- [5] Birhane, A., Prabhu, V.U., Kahembwe, E.: Multimodal datasets: misogyny, pornography, and malignant stereotypes. arXiv preprint arXiv:2110.01963 (2021)
- [6] Blattmann, A., Dockhorn, T., Kulal, S., Mendelevitch, D., Kilian, M., Lorenz, D., Levi, Y., English, Z., Voleti, V., Letts, A., Jampani, V., Rombach, R.: Stable Video Diffusion: Scaling latent video diffusion models to large datasets. arXiv preprint arXiv:2311.15127 (2023)
- [7] Bugliarello, E., Moraldo, H., Villegas, R., Babaeizadeh, M., Saffar, M.T., Zhang, H., Erhan, D., Ferrari, V., Kindermans, P.J., Voigtlaender, P.: StoryBench: A multifaceted benchmark for continuous story visualization. In: NeurIPS D&B (2023)
- [8] Cao, H., Tan, C., Gao, Z., Xu, Y., Chen, G., Heng, P.A., Li, S.Z.: A survey on generative diffusion models. IEEE Trans Knowl. Data Eng. **36**(7) (2024)
- [9] Carreira, J., Noland, E., Banki-Horvath, A., Hillier, C., Zisserman, A.: A short note about kinetics-600. arXiv preprint arXiv:1808.01340 (2018)
- [10] Carreira, J., Zisserman, A.: Quo vadis, action recognition? A new model and the kinetics dataset. In: CVPR (2017)
- [11] Castellano, B.: PySceneDetect (2024)
- [12] Chan, C., Ginosar, S., Zhou, T., Efros, A.A.: Everybody dance now. In: ICCV (2019)
- [13] Chang, D., Shi, Y., Gao, Q., Xu, H., Fu, J., Song, G., Yan, Q., Zhu, Y., Yang, X., Soleymani, M.: MagicPose: Realistic human poses and facial expressions retargeting with identity-aware diffusion. In: ICML (2024)
- [14] Chefer, H., Zada, S., Paiss, R., Ephrat, A., Tov, O., Rubinstein, M., Wolf, L., Dekel, T., Michaeli, T., Mosseri, I.: Still-moving: Customized video generation without customized video data. arXiv preprint arXiv:2407.08674 (2024)
- [15] Chen, C., Shu, J., Chen, L., He, G., Wang, C., Li, Y.: Motion-Zero: Zero-shot moving object control framework for diffusion-based video generation. arXiv preprint arXiv:2401.10150 (2024)
- [16] Chen, T.S., Siarohin, A., Menapace, W., Deyneka, E., Chao, H.w., Jeon, B.E., Fang, Y., Lee, H.Y., Ren, J., Yang, M.H., Tulyakov, S.: Panda-70M: Captioning 70m videos with multiple cross-modality teachers. In: CVPR (2024)

- [17] Chen, W., Ji, Y., Wu, J., Wu, H., Xie, P., Li, J., Xia, X., Xiao, X., Lin, L.: Control-A-Video: Controllable text-to-video generation with diffusion models. arXiv preprint arXiv:2305.13840 (2023)
- [18] Cohen, N., Kulikov, V., Kleiner, M., Huberman-Spiegelglas, I., Michaeli, T.: Slicedit: Zero-shot video editing with text-to-image diffusion models using spatio-temporal slices. In: Salakhutdinov, R., Kolter, Z., Heller, K., Weller, A., Oliver, N., Scarlett, J., Berkenkamp, F. (eds.) ICML. vol. 235 (2024)
- [19] Croitoru, F.A., Hondru, V., Ionescu, R.T., Shah, M.: Diffusion models in vision: A survey. IEEE TPAMI **45**(9) (2023)
- [20] Deep Vision Lab, T.C.U.o.H.K.: ControlNeXt (2024), <https://github.com/dvlab-research/ControlNeXt/blob/ab4b3acf912ccc178d23bbf003369dfb657fc8d01/ControlNeXt-SVD-v2/dwpose/preprocess.py>
- [21] Eigen, D., Puhrsch, C., Fergus, R.: Depth map prediction from a single image using a multi-scale deep network. In: NeurIPS (2014)
- [22] Epstein, D., Chen, B., Vondrick, C.: Oops! predicting unintentional action in video. In: CVPR (2020)
- [23] Gao, Y., Liu, J., Xu, Z., Zhang, J., Li, K., Ji, R., Shen, C.: PyramidCLIP: Hierarchical feature alignment for vision-language model pretraining. In: Oh, A.H., Agarwal, A., Belgrave, D., Cho, K. (eds.) NeurIPS (2022)
- [24] Gemini Team Google: Gemini: A family of highly capable multimodal models. arXiv preprint arXiv:2312.11805 (2023)
- [25] Geyer, M., Bar-Tal, O., Bagon, S., Dekel, T.: Tokenflow: Consistent diffusion features for consistent video editing. arXiv preprint arXiv:2307.10373 (2023)
- [26] Guo, Y., Yang, C., Rao, A., Agrawala, M., Lin, D., Dai, B.: SparseCtrl: Adding sparse controls to text-to-video diffusion models. arXiv preprint arXiv:2311.16933 (2023)
- [27] He, H., Xu, Y., Guo, Y., Wetzstein, G., Dai, B., Li, H., Yang, C.: CameraCtrl: Enabling camera control for text-to-video generation. arXiv preprint arXiv:2404.02101 (2024)
- [28] He, X., Jiang, D., Zhang, G., Ku, M., Soni, A., Siu, S., Chen, H., Chandra, A., Jiang, Z., Arulraj, A., Wang, K., Do, Q.D., Ni, Y., Lyu, B., Narsupalli, Y., Fan, R., Lyu, Z., Lin, Y., Chen, W.: VideoScore: Building automatic metrics to simulate fine-grained human feedback for video generation. arXiv preprint arXiv:2406.15252 (2024)
- [29] Hendricks, L.A., Wang, O., Shechtman, E., Sivic, J., Darrell, T., Russell, B.: Localizing moments in video with natural language. In: ICCV (2017)
- [30] Heusel, M., Ramsauer, H., Unterthiner, T., Nessler, B., Hochreiter, S.: Gans trained by a two time-scale update rule converge to a local nash equilibrium. In: Guyon, I., Luxburg, U.V., Bengio, S., Wallach, H., Fergus, R., Vishwanathan, S., Garnett, R. (eds.) NeurIPS. vol. 30. Curran Associates, Inc. (2017)
- [31] Ho, J., Chan, W., Saharia, C., Whang, J., Gao, R., Gritsenko, A., Kingma, D.P., Poole, B., Norouzi, M., Fleet, D.J., Salimans, T.: Imagen Video: High definition video generation with diffusion models. arXiv preprint arXiv:2210.02303 (2022)

- [32] Ho, J., Jain, A., Abbeel, P.: Denoising diffusion probabilistic models. In: Larochelle, H., Ranzato, M., Hadsell, R., Balcan, M., Lin, H. (eds.) *NeurIPS*. vol. 33 (2020)
- [33] Ho, J., Salimans, T., Gritsenko, A.A., Chan, W., Norouzi, M., Fleet, D.J.: Video diffusion models. In: Oh, A.H., Agarwal, A., Belgrave, D., Cho, K. (eds.) *NeurIPS* (2022)
- [34] Hong, W., Ding, M., Zheng, W., Liu, X., Tang, J.: CogVideo: Large-scale pretraining for text-to-video generation via transformers. *arXiv preprint arXiv:2205.15868* (2022)
- [35] Hu, L., Gao, X., Zhang, P., Sun, K., Zhang, B., Bo, L.: Animate Anyone: Consistent and controllable image-to-video synthesis for character animation. *arXiv preprint arXiv:2311.17117* (2023)
- [36] Hu, Y., Luo, C., Chen, Z.: Make it move: Controllable image-to-video generation with text descriptions. In: *CVPR* (2022)
- [37] Huang, K., Sun, K., Xie, E., Li, Z., Liu, X.: T2I-CompBench: A comprehensive benchmark for open-world compositional text-to-image generation. In: *NeurIPS D&B* (2023)
- [38] Huang, Z., He, Y., Yu, J., Zhang, F., Si, C., Jiang, Y., Zhang, Y., Wu, T., Jin, Q., Chanpaisit, N., Wang, Y., Chen, X., Wang, L., Lin, D., Qiao, Y., Liu, Z.: VBench: Comprehensive benchmark suite for video generative models. In: *CVPR* (2024)
- [39] Jafarian, Y., Park, H.S.: Learning high fidelity depths of dressed humans by watching social media dance videos. In: *CVPR* (2021)
- [40] Jain, Y., Nasery, A., Vineet, V., Behl, H.: PEEKABOO: Interactive video generation via masked-diffusion. In: *CVPR* (2024)
- [41] Kajic, I., Wiles, O., Albuquerque, I., Bauer, M., Wang, S., Pont-Tuset, J., Nematzadeh, A.: Evaluating numerical reasoning in text-to-image models. In: *NeurIPS D&B* (2024)
- [42] Karras, J., Holynski, A., Wang, T.C., Kemelmacher-Shlizerman, I.: DreamPose: Fashion video synthesis with stable diffusion. In: *ICCV* (2023)
- [43] Kay, W., Carreira, J., Simonyan, K., Zhang, B., Hillier, C., Vijayanarasimhan, S., Viola, F., Green, T., Back, T., Natsev, A., Suleyman, M., Zisserman, A.: The kinetics human action video dataset. *arXiv preprint arXiv:1705.06950* (2017)
- [44] Kim, J., Kim, M.J., Lee, J., Choo, J.: Tcan: Animating human images with temporally consistent pose guidance using diffusion models. In: Leonardi, A., Ricci, E., Roth, S., Russakovsky, O., Sattler, T., Varol, G. (eds.) *ECCV*. Cham (2024)
- [45] Kirstain, Y., Polyak, A., Singer, U., Matiana, S., Penna, J., Levy, O.: Pick-a-pic: An open dataset of user preferences for text-to-image generation. In: *NeurIPS* (2023)
- [46] Kondratyuk, D., Yu, L., Gu, X., Lezama, J., Huang, J., Schindler, G., Hornung, R., Birodkar, V., Yan, J., Chiu, M.C., Somandepalli, K., Akbari, H., Alon, Y., Cheng, Y., Dillon, J., Gupta, A., Hahn, M., Hauth, A., Hendon, D., Martinez, A., Minnen, D., Sirotenko, M., Sohn, K., Yang, X., Adam, H., Yang, M.H., Essa, I., Wang, H., Ross, D.A., Seybold, B., Jiang, L.: VideoPoet: A large language model for zero-shot video generation. In: *ICML* (2024)
- [47] Lei, W., Wang, J., Ma, F., Huang, G., Liu, L.: A comprehensive survey on human video generation: Challenges, methods, and insights. *arXiv preprint arXiv:2407.08428* (2024)



- [48] Li, Z., Swanson, K., Bampis, C., Krasula, L., Aaron, A.: Toward a better quality metric for the video community. <https://netflixtechblog.com/toward-a-better-quality-metric-for-the-video-community-7ed94e752a30> (2020), accessed: Mar 3, 2025
- [49] Lin, H., Cho, J., Zala, A., Bansal, M.: Ctrl-adapter: An efficient and versatile framework for adapting diverse controls to any diffusion model. arXiv preprint arXiv:2404.09967 (2024)
- [50] Lin, Z., Pathak, D., Li, B., Li, J., Xia, X., Neubig, G., Zhang, P., Ramanan, D.: Evaluating text-to-visual generation with image-to-text generation. In: arXiv preprint arXiv:2404.01291 (2024)
- [51] Lipman, Y., Chen, R.T.Q., Ben-Hamu, H., Nickel, M., Le, M.: Flow matching for generative modeling. In: ICLR (2023)
- [52] Liu, F., Bugliarello, E., Ponti, E.M., Reddy, S., Collier, N., Elliott, D.: Visually grounded reasoning across languages and cultures. In: EMNLP. Online and Punta Cana, Dominican Republic (2021)
- [53] Liu, W., Piao, Z., Min, J., Luo, W., Ma, L., Gao, S.: Liquid warping gan: A unified framework for human motion imitation, appearance transfer and novel view synthesis. In: ICCV (2019)
- [54] Liu, Y., Cun, X., Liu, X., Wang, X., Zhang, Y., Chen, H., Liu, Y., Zeng, T., Chan, R., Shan, Y.: EvalCrafter: Benchmarking and evaluating large video generation models. arXiv preprint arXiv:2310.11440 (2023)
- [55] Lu, W., Xu, Y., Zhang, J., Wang, C., Tao, D.: HandRefiner: Refining malformed hands in generated images by diffusion-based conditional inpainting. In: ACM-MM (2024)
- [56] Luo, X., Zhan, R., Chang, H., Yang, F., Milanfar, P.: Distortion agnostic deep watermarking. In: CVPR (2020)
- [57] Ma, Y., He, Y., Cun, X., Wang, X., Chen, S., Li, X., Chen, Q.: Follow your pose: Pose-guided text-to-video generation using pose-free videos. AAAI **38**(5) (2024)
- [58] Meister, N., Zhao, D., Wang, A., Ramaswamy, V.V., Fong, R., Russakovsky, O.: Gender artifacts in visual datasets. arXiv preprint arXiv:2206.09191 (2022)
- [59] Minderer, M., Gritsenko, A.A., Houlsby, N.: Scaling open-vocabulary object detection. In: NeurIPS (2023)
- [60] Ni, H., Shi, C., Li, K., Huang, S.X., Min, M.R.: Conditional image-to-video generation with latent flow diffusion models. In: CVPR (2023)
- [61] Oquab, M., Darcet, T., Moutakanni, T., Vo, H., Szafraniec, M., Khalidov, V., Fernandez, P., Haziza, D., Massa, F., El-Nouby, A., Assran, M., Ballas, N., Galuba, W., Howes, R., Huang, P.Y., Li, S.W., Misra, I., Rabbat, M., Sharma, V., Synnaeve, G., Xu, H., Jegou, H., Mairal, J., Labatut, P., Joulin, A., Bojanowski, P.: DINOv2: Learning robust visual features without supervision. TMLR (2024)
- [62] Peng, B., Wang, J., Zhang, Y., Li, W., Yang, M.C., Jia, J.: ControlNeXt: Powerful and efficient control for image and video generation. arXiv preprint arXiv:2408.06070 (2024)
- [63] Podell, D., English, Z., Lacey, K., Blattmann, A., Dockhorn, T., Müller, J., Penna, J., Rombach, R.: Sdxl: Improving latent diffusion models for high-resolution image synthesis. In: arXiv preprint arXiv:2307.01952 (2023)

- [64] Polyak, A., Zohar, A., Brown, A., Tjandra, A., Sinha, A., Lee, A., Vyas, A., Shi, B., Ma, C.Y., Chuang, C.Y., Yan, D., Choudhary, D., Wang, D., Sethi, G., Pang, G., Ma, H., Misra, I., Hou, J., Wang, J., Jagadeesh, K., Li, K., Zhang, L., Singh, M., Williamson, M., Le, M., Yu, M., Singh, M.K., Zhang, P., Vajda, P., Duval, Q., Girdhar, R., Sumbaly, R., Rambhatla, S.S., Tsai, S., Azadi, S., Datta, S., Chen, S., Bell, S., Ramaswamy, S., Sheynin, S., Bhattacharya, S., Motwani, S., Xu, T., Li, T., Hou, T., Hsu, W.N., Yin, X., Dai, X., Taigman, Y., Luo, Y., Liu, Y.C., Wu, Y.C., Zhao, Y., Kirstain, Y., He, Z., He, Z., Pumarola, A., Thabet, A., Sanakoyeu, A., Mallya, A., Guo, B., Araya, B., Kerr, B., Wood, C., Liu, C., Peng, C., Vengertsev, D., Schonfeld, E., Blanchard, E., Juefei-Xu, F., Nord, F., Liang, J., Hoffman, J., Kohler, J., Fire, K., Sivakumar, K., Chen, L., Yu, L., Gao, L., Georgopoulos, M., Moritz, R., Sampson, S.K., Li, S., Parmeggiani, S., Fine, S., Fowler, T., Petrovic, V., Du, Y.: Movie Gen: A cast of media foundation models. arXiv preprint arXiv:2410.13720 (2024)
- [65] Pont-Tuset, J., Perazzi, F., Caelles, S., Arbeláez, P., Sorkine-Hornung, A., Van Gool, L.: The 2017 DAVIS challenge on video object segmentation. arXiv:1704.00675 (2017)
- [66] Pouget, A., Beyer, L., Bugliarello, E., Wang, X., Steiner, A., Zhai, X., Alabdulmohsin, I.: No filter: Cultural and socioeconomic diversity in contrastive vision-language models. In: Globerson, A., Mackey, L., Belgrave, D., Fan, A., Paquet, U., Tomczak, J., Zhang, C. (eds.) NeurIPS. vol. 37 (2024)
- [67] Ravi, N., Gabeur, V., Hu, Y.T., Hu, R., Ryali, C., Ma, T., Khedr, H., Rädle, R., Rolland, C., Gustafson, L., Mintun, E., Pan, J., Alwala, K.V., Carion, N., Wu, C.Y., Girshick, R., Dollar, P., Feichtenhofer, C.: SAM 2: Segment anything in images and videos. In: The Thirteenth International Conference on Learning Representations (2025)
- [68] Ren, W., Yang, H., Zhang, G., Wei, C., Du, X., Huang, S., Chen, W.: Consisti2v: Enhancing visual consistency for image-to-video generation. arXiv preprint arXiv:2402.04324 (2024)
- [69] Ren, Y., Li, G., Liu, S., Li, T.H.: Deep spatial transformation for pose-guided person image generation and animation. IEEE TIP **29** (2020)
- [70] Shi, X., Huang, Z., Wang, F.Y., Bian, W., Li, D., Zhang, Y., Zhang, M., Cheung, K.C., See, S., Qin, H., Dai, J., Li, H.: Motion-I2V: Consistent and controllable image-to-video generation with explicit motion modeling. In: ACM SIGGRAPH. New York, NY, USA (2024)
- [71] Siarohin, A., Woodford, O.J., Ren, J., Chai, M., Tulyakov, S.: Motion representations for articulated animation. In: CVPR (2021)
- [72] Singer, U., Polyak, A., Hayes, T., Yin, X., An, J., Zhang, S., Hu, Q., Yang, H., Ashual, O., Gafni, O., et al.: Make-A-Video: Text-to-video generation without text-video data. arXiv preprint arXiv:2209.14792 (2022)
- [73] Singer, U., Zohar, A., Kirstain, Y., Sheynin, S., Polyak, A., Parikh, D., Taigman, Y.: Video editing via factorized diffusion distillation. In: ECCV. Springer (2024)
- [74] Soomro, K., Zamir, A.R., Shah, M.: UCF101: A dataset of 101 human actions classes from videos in the wild. arXiv preprint arXiv:1212.0402 (2012)
- [75] Stein, G., Cresswell, J., Hosseinzadeh, R., Sui, Y., Ross, B., Vilecroze, V., Liu, Z., Caterini, A.L., Taylor, E., Loaiza-Ganem, G.: Exposing flaws of generative model evaluation metrics and their unfair treatment of diffusion models. In: Oh, A., Naumann, T., Globerson, A., Saenko, K., Hardt, M., Levine, S. (eds.) NeurIPS. vol. 36 (2023)

- [76] Teed, Z., Deng, J.: Raft: Recurrent all-pairs field transforms for optical flow. In: ECCV (2020)
- [77] Tencent: MimicMotion (2024), <https://github.com/Tencent/MimicMotion/blob/62f91e1f4ab750e1ab0d96c08f2d199b6e84e8b1/mimicmotion/dwpose/preprocess.py>
- [78] Tulyakov, S., Liu, M.Y., Yang, X., Kautz, J.: Mocogan: Decomposing motion and content for video generation. In: CVPR (2018)
- [79] Unterthiner, T., van Steenkiste, S., Kurach, K., Marinier, R., Michalski, M., Gelly, S.: FVD: A new metric for video generation. In: DGS@ICLR (2019)
- [80] Villegas, R., Babaeizadeh, M., Kindermans, P.J., Moraldo, H., Zhang, H., Saffar, M.T., Castro, S., Kunze, J., Erhan, D.: Phenaki: Variable length video generation from open domain textual descriptions. In: ICLR (2023)
- [81] Voigtlaender, P., Changpinyo, S., Pont-Tuset, J., Soricut, R., Ferrari, V.: Connecting vision and language with video localized narratives. In: CVPR (2023)
- [82] Wang, J., Zhang, Y., Zou, J., Zeng, Y., Wei, G., Yuan, L., Li, H.: Boximator: Generating rich and controllable motions for video synthesis. arXiv preprint arXiv:2402.01566 (2024)
- [83] Wang, T., Li, L., Lin, K., Zhai, Y., Lin, C.C., Yang, Z., Zhang, H., Liu, Z., Wang, L.: DiSco: Disentangled control for realistic human dance generation. In: CVPR (2024)
- [84] Wang, X., Yuan, H., Zhang, S., Chen, D., Wang, J., Zhang, Y., Shen, Y., Zhao, D., Zhou, J.: Videocomposer: Compositional video synthesis with motion controllability. In: NeurIPS (2023)
- [85] Wang, X., Zhang, S., Yuan, H., Qing, Z., Gong, B., Zhang, Y., Shen, Y., Gao, C., Sang, N.: A recipe for scaling up text-to-video generation with text-free videos. In: CVPR (2024)
- [86] Wang, Y., Ma, X., Chen, X., Chen, C., Dantcheva, A., Dai, B., Qiao, Y.: Leo: Generative latent image animator for human video synthesis. IJCV (2024)
- [87] Wang, Z., Li, Y., Zeng, Y., Fang, Y., Guo, Y., Liu, W., Tan, J., Chen, K., Xue, T., Dai, B., Lin, D.: HumanVid: Demystifying training data for camera-controllable human image animation. In: Globerson, A., Mackey, L., Belgrave, D., Fan, A., Paquet, U., Tomczak, J., Zhang, C. (eds.) NeurIPS D&B. vol. 37 (2024)
- [88] Wang, Z.: Image quality assessment: from error visibility to structural similarity. IEEE TIP **13**(4) (2004)
- [89] Wang, Z., Yuan, Z., Wang, X., Chen, T., Xia, M., Luo, P., Shan, Y.: MotionCtrl: A unified and flexible motion controller for video generation. In: arXiv preprint arXiv:2312.03641 (2023)
- [90] Wiles, O., Zhang, C., Albuquerque, I., Kajic, I., Wang, S., Bugliarello, E., Onoe, Y., Papalampidi, P., Ktena, I., Knutsen, C., Rashtchian, C., Nawalgaria, A., Pont-Tuset, J., Nematzadeh, A.: Revisiting text-to-image evaluation with gecko: on metrics, prompts, and human rating. In: ICLR (2025)
- [91] Wu, J.Z., Fang, G., Wu, H., Wang, X., Ge, Y., Cun, X., Zhang, D.J., Liu, J.W., Gu, Y., Zhao, R., Lin, W., Hsu, W., Shan, Y., Shou, M.Z.: Towards a better metric for text-to-video generation. arXiv preprint arXiv:2401.07781 (2024)
- [92] Wu, J.Z., Ge, Y., Wang, X., Lei, S.W., Gu, Y., Shi, Y., Hsu, W., Shan, Y., Qie, X., Shou, M.Z.: Tune-A-Video: One-shot tuning of image diffusion models for text-to-video generation. In: ICCV (2023)

- [93] Xing, J., Xia, M., Liu, Y., Zhang, Y., Zhang, Y., He, Y., Liu, H., Chen, H., Cun, X., Wang, X., Shan, Y., Wong, T.T.: Make-Your-Video: Customized video generation using textual and structural guidance. arXiv preprint arXiv:2306.00943 (2023)
- [94] Xing, J., Xia, M., Zhang, Y., Chen, H., Yu, W., Liu, H., Liu, G., Wang, X., Shan, Y., Wong, T.T.: DynamiCrafter: Animating open-domain images with video diffusion priors. In: ECCV (2024)
- [95] Xu, J., Mei, T., Yao, T., Rui, Y.: MSR-VTT: A large video description dataset for bridging video and language. In: CVPR (2016)
- [96] Xu, Z., Zhang, J., Liew, J.H., Yan, H., Liu, J.W., Zhang, C., Feng, J., Shou, M.Z.: MagicAnimate: Temporally consistent human image animation using diffusion model. In: CVPR (2024)
- [97] Ya, G., Favero, G., Luo, Z.H., Jolicoeur-Martineau, A., Pal, C., et al.: Beyond FVD: Enhanced evaluation metrics for video generation quality. arXiv preprint arXiv:2410.05203 (2024)
- [98] Yang, L., Kang, B., Huang, Z., Zhao, Z., Xu, X., Feng, J., Zhao, H.: Depth anything v2. arXiv:2406.09414 (2024)
- [99] Yang, S., Hou, L., Huang, H., Ma, C., Wan, P., Zhang, D., Chen, X., Liao, J.: Direct-a-Video: Customized video generation with user-directed camera movement and object motion. In: ACM SIGGRAPH 2024 Conference Papers. New York, NY, USA (2024)
- [100] Yang, Z., Zeng, A., Yuan, C., Li, Y.: Effective whole-body pose estimation with two-stages distillation. In: ICCV Workshops (2023)
- [101] Yin, S., Wu, C., Liang, J., Shi, J., Li, H., Ming, G., Duan, N.: Dragnuwa: Fine-grained control in video generation by integrating text, image, and trajectory. arXiv preprint arXiv:2308.08089 (2023)
- [102] Zhang, D.J., Li, D., Le, H., Shou, M.Z., Xiong, C., Sahoo, D.: Moonshot: Towards controllable video generation and editing with multimodal conditions. arXiv preprint arXiv:2401.01827 (2024)
- [103] Zhang, M., Fu, Y., Ding, Z., Liu, S., Tu, Z., Wang, X.: Hoidiffusion: Generating realistic 3d hand-object interaction data. In: CVPR (2024)
- [104] Zhang, P., Yang, L., Lai, J.H., Xie, X.: Exploring dual-task correlation for pose guided person image generation. In: CVPR (2022)
- [105] Zhang, R., Isola, P., Efros, A.A., Shechtman, E., Wang, O.: The unreasonable effectiveness of deep features as a perceptual metric. In: CVPR (2018)
- [106] Zhang, Y., Wei, Y., Jiang, D., Zhang, X., Zuo, W., Tian, Q.: ControlVideo: Training-free controllable text-to-video generation. arXiv preprint arXiv:2305.13077 (2023)
- [107] Zhang, Y., Gu, J., Wang, L.W., Wang, H., Cheng, J., Zhu, Y., Zou, F.: MimicMotion: High-quality human motion video generation with confidence-aware pose guidance. arXiv preprint arXiv:2406.19680 (2024)

## Overview

Our Appendix includes the following content as follows.

Appendix A shows videos generated by our seven models. Fig. 11 (p. 22) shows how the extracted poses influence MagicAnimate’s video generation. Figs. 12 to 26 (pp. 24–38) show samples generated by all the models for five examples.

Appendix B (pp. 38–45) provides further details from our data preparation pipeline. Fig. 27 shows a high-level overview of the filtering process. Tabs. 4 and 5 list additional details of the dataset construction (p. 38), while Figs. 36 and 37 compare video duration and resolution across the WYD, TikTok and TED-Talks datasets (p. 43). Figs. 28 to 34 (pp. 39–42) show sample videos that were removed as part of the filtering process, and Fig. 35 (p. 42) shows more examples from the final WYD dataset. Figs. 38 and 39 (pp. 43–44) show our UIs for video categorization and segmentation. Fig. 40 displays the overlap in videos between any two categories.

Appendix C reports additional results from our experiments. Fig. 41 (p. 46) shows the difference in errors of depth- and edge-conditioned models when adding captions as an additional source of guidance. Figs. 42 to 45 (pp. 46–49) report and discuss category-level performance of our top-performing models (MimicMotion, ControlNeXt and TF-T2V) w.r.t. sample-level metrics (ICD, OFE, pICD, pAPE).

Appendix D includes further details from our evaluations. We report our instructions and setup for side-by-side human evaluations in p. 50, and show our UI in Fig. 50 (p. 52). Figs. 46 to 49 (pp. 51–52) present and discuss how all the metrics that we considered to measure different aspects of video generation score our seven evaluated models.

Finally, we share some ethical considerations related to controllable human video generation in Appendix E (p. 33), where we additionally remark that our WYD dataset is meant to be used for academic research purposes only.

Model	Condition	Extractor	Training data	Close-up single-person videos?	WYD overlap?
MagicAnimate [96]	Dense pose	Detectron2	TikTok [39]	Yes	No
MagicPose [13]	2D pose	OpenPose	TikTok [39]	Yes	No
MimicMotion [107]	2D pose	DWPose	Internal	Yes	No
ControlNeXt-SVD-v2 [62]	2D pose	DWPose	N/A	N/A	N/A
Control-A-Video [17]	Depth / Canny	MiDaS / OpenCV	WebVid [1] subset* + internal	No	No
TF-T2V [85]	Depth	MiDaS	WebVid [1] subset* + internal	No	No
Ctrl-Adapter [49]	Depth / Canny	MiDaS / OpenCV	Panda-70M [16]	No	No

Table 3 | **Overview of evaluated models.** We list models’ conditions and used extractors, their training data and whether it mostly consists of close-up single-person videos, and whether any of the video datasets used in WYD were used by them during training. We thank the authors for clarifying information about their training data and confirming the absence of overlap with our evaluation videos. \* Note that different models rely on different subsets of WebVid.

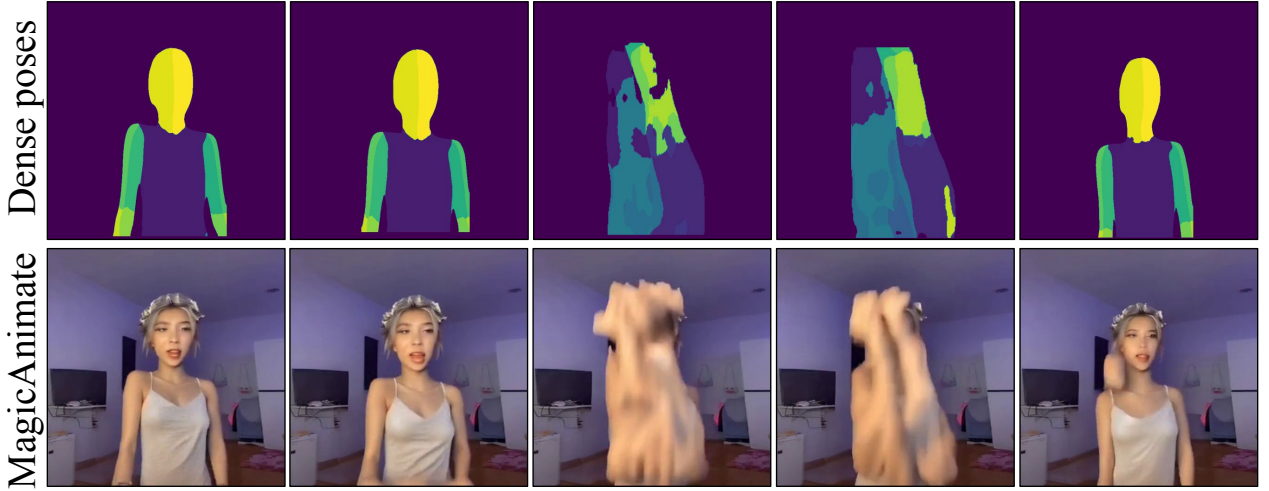


Figure 11 | MagicAnimate generations and their dense poses (conditioning signal) in TikTok.

## A. Samples of generated videos

An overview of the evaluated models is shown in Tab. 3. We show how the quality of poses extracted from the reference video influence MagicAnimate’s video generation in Fig. 11. Figs. 12 to 26 show and discuss the limitations of samples generated by all the models for five WYD examples.



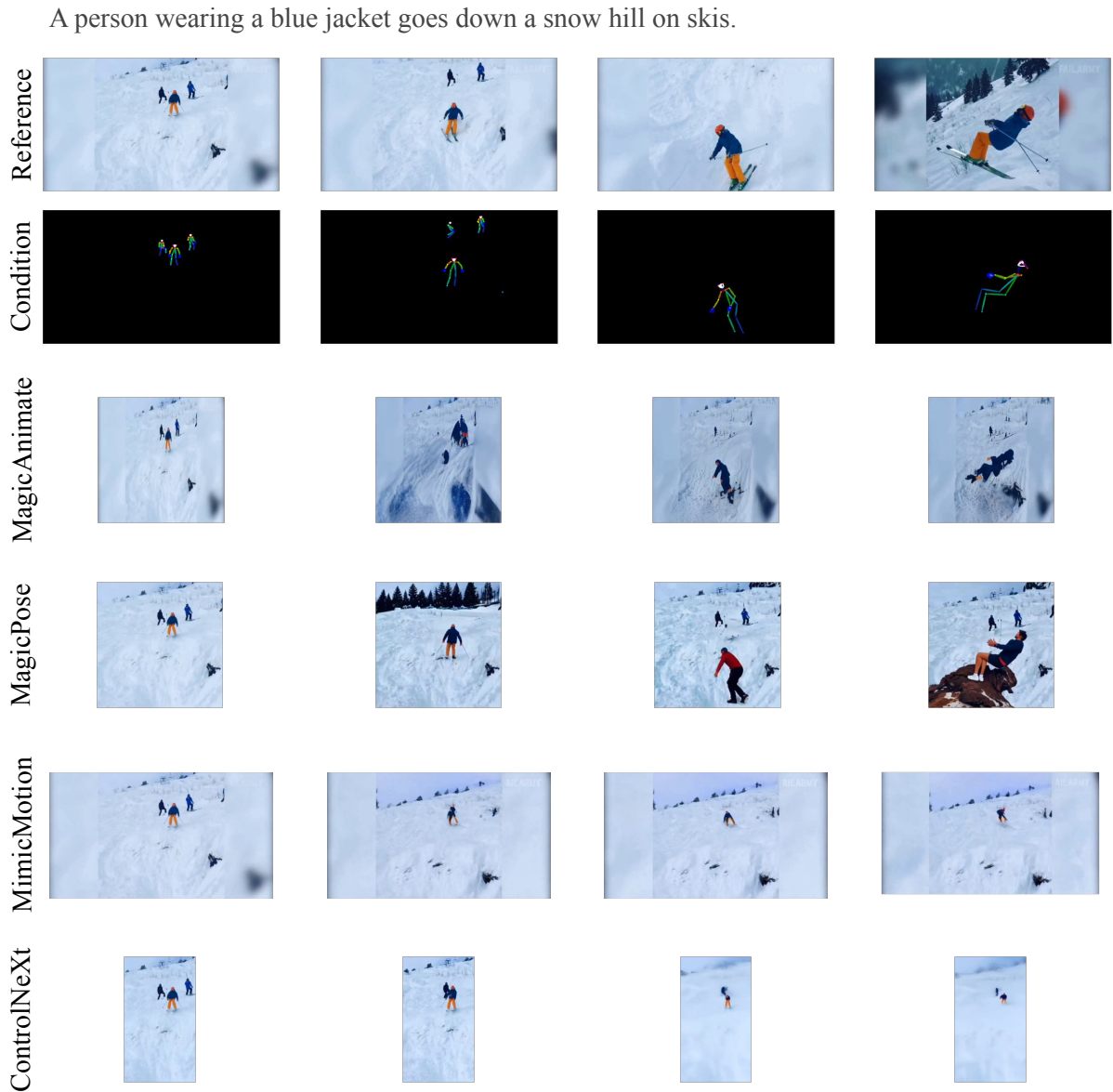


Figure 12 | Example generations of our evaluated pose-conditioned models (MagicAnimate uses dense poses). We can see how people’s appearance changes in MagicPose, although matching the human movements the best. We can also see the size mismatches in ControlNeXt and MimicMotion.

A person wearing a blue jacket goes down a snow hill on skis.

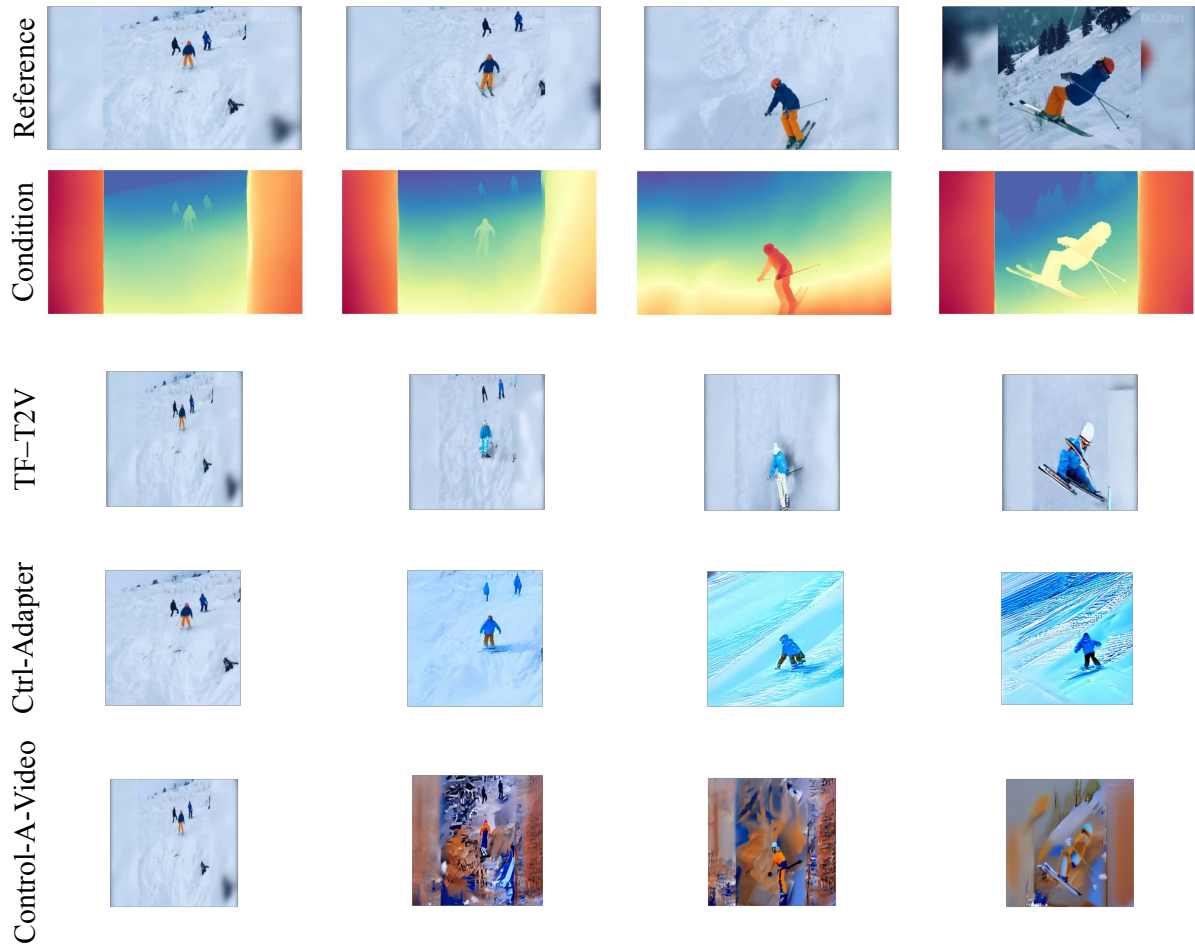


Figure 13 | Example generations of our evaluated depth-conditioned models. We can see how people’s appearance changes in TF-T2V, increasing saturation in Ctrl-Adapter and distortions in Control-A-Video.

A person wearing a blue jacket goes down a snow hill on skis.

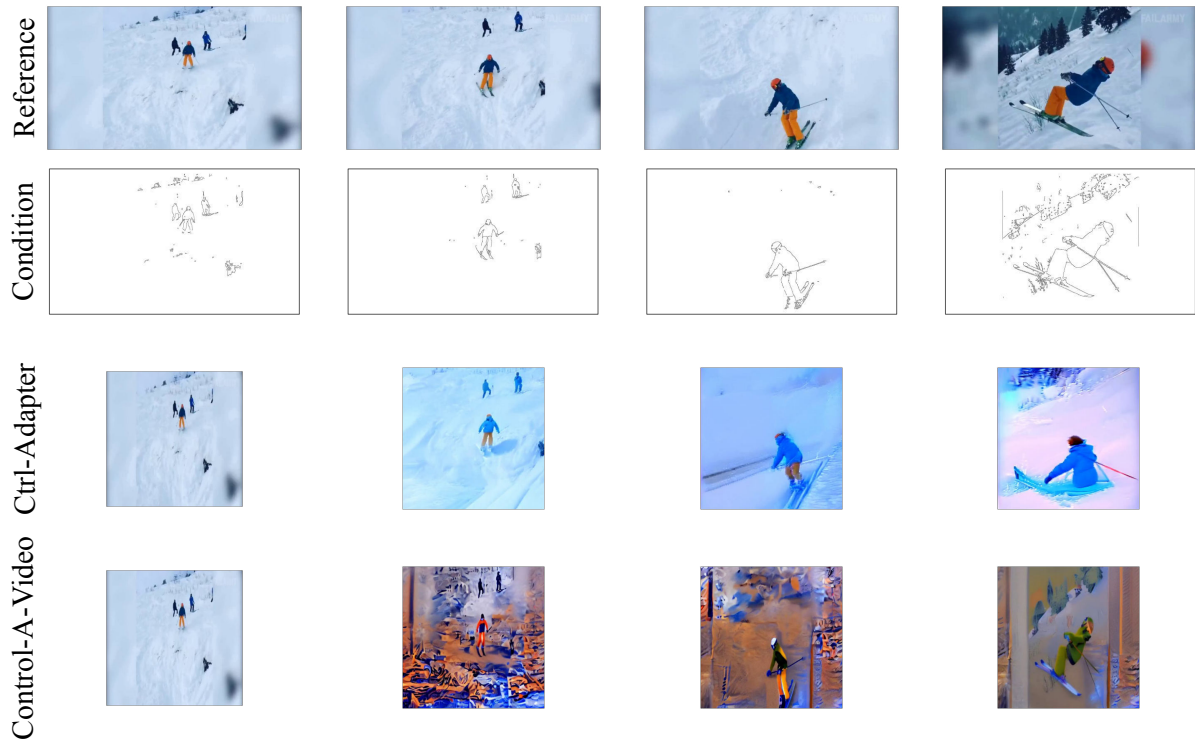


Figure 14 | Example generations of our evaluated edge-conditioned models. We can see increasing saturation in Ctrl-Adapter and distortions in Control-A-Video.



Figure 15 | Example generations of our evaluated pose-conditioned models (MagicAnimate uses dense poses). We note the challenges in camera motion for all models, the distortions of characters in MagicAnimate, and flickering effects in MagicPose, as well as horse disappearance in MimicMotion.

A woman wearing a white top is riding a brown horse while horses are standing on the brown surface.

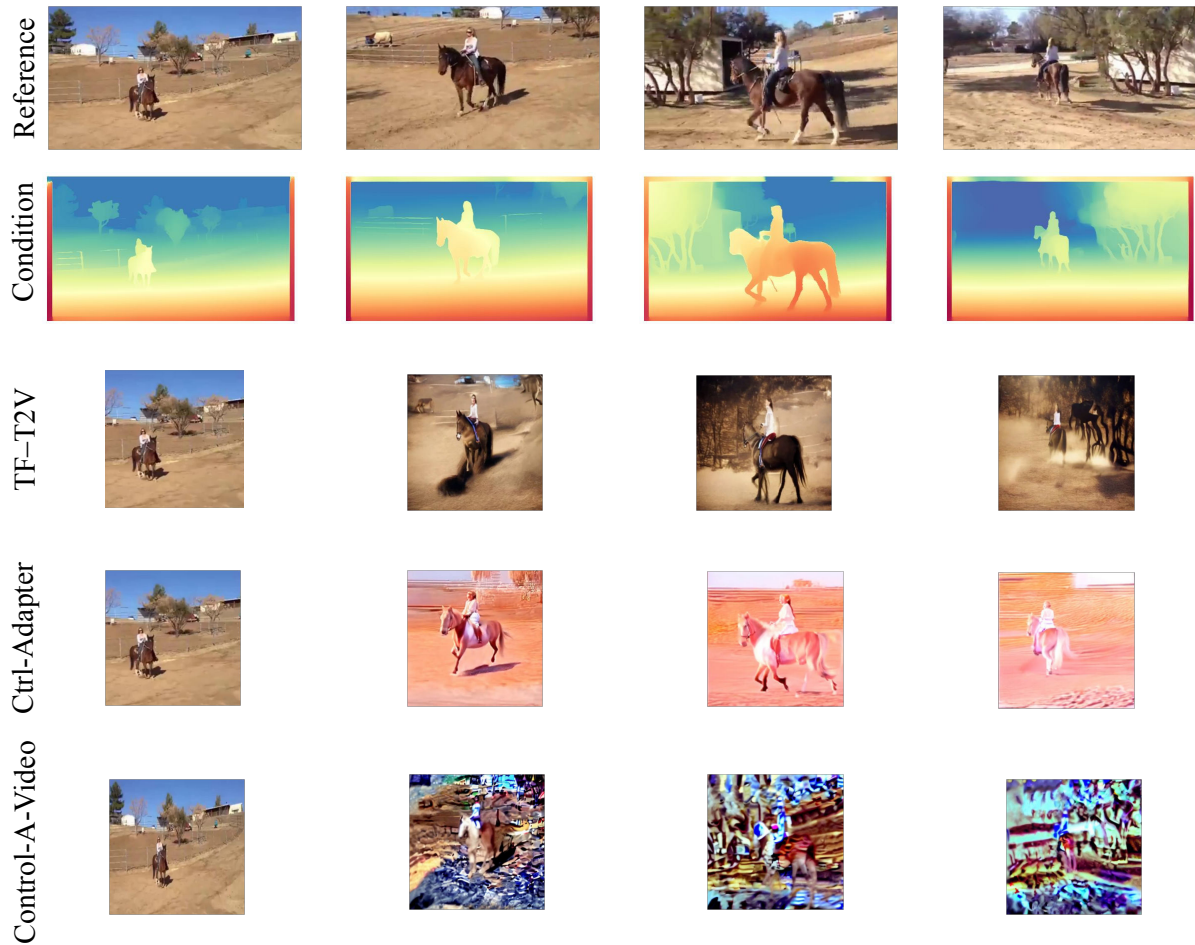


Figure 16 | Example generations of our evaluated depth-conditioned models. We can see increasing saturation in Ctrl-Adapter and distortions in Control-A-Video, while TF-T2V best matches the overall scene.



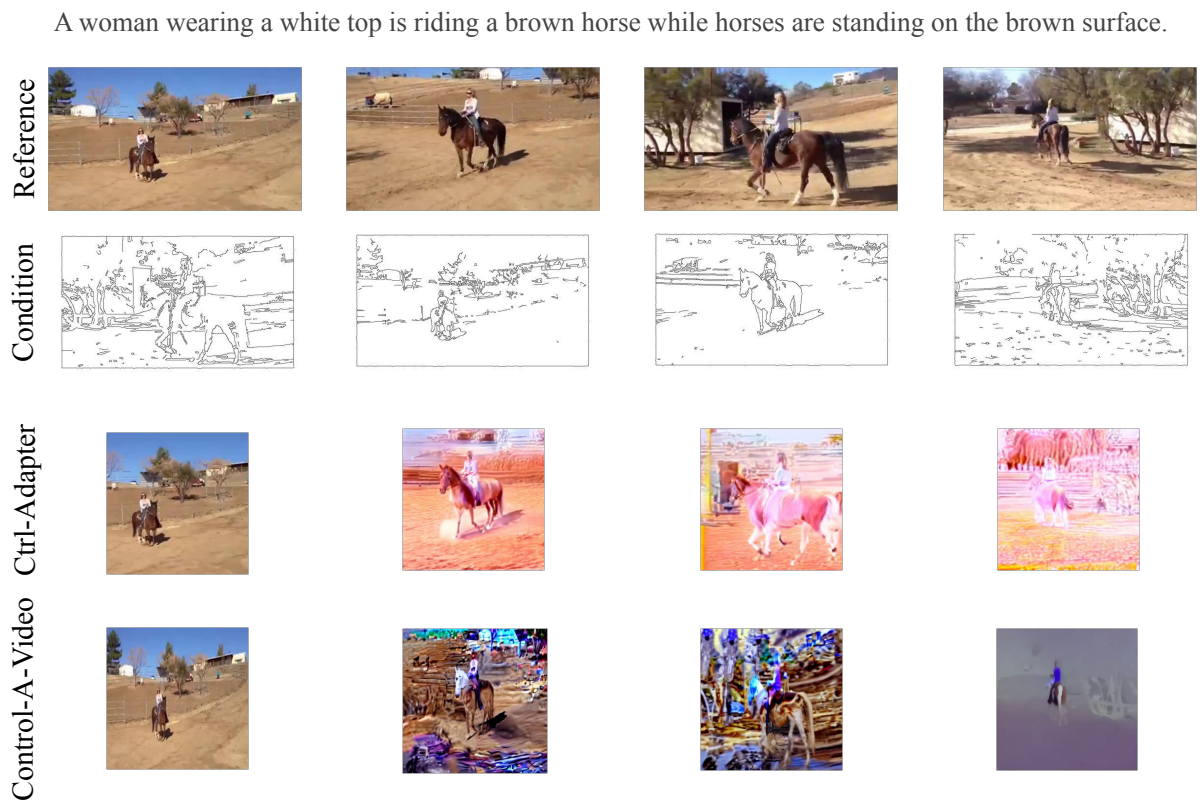


Figure 17 | Example generations of our evaluated edge-conditioned models. We can see increasing saturation in Ctrl-Adapter and distortions in Control-A-Video.





Figure 18 | Example generations of our evaluated pose-conditioned models (MagicAnimate uses dense poses). We can see how MimicMotion changes the facial traits of humans towards specific age and beauty standards, and how it also fails to make the man interact with the pan. Due to its pre-processing, ControlNeXt misses the face of the man in the first frame and later creates a different one.



Figure 19 | Example generations of our evaluated depth-conditioned models. We can see how Ctrl-Adapter change the facial traits of humans towards specific age and beauty standards. We can still see increasing saturation in Ctrl-Adapter and distortions in Control-A-Video, although less than in previous, dynamic examples.



Figure 20 | Example generations of our evaluated edge-conditioned models. Similar to their depth-conditioned counterparts, Ctrl-Adapter shows increasing saturation and Control-A-Video presents distortions.



Figure 21 | Example generations of our evaluated pose-conditioned models (MagicAnimate uses dense poses). Besides the large distortions and artifacts in MagicAnimate, all pose-conditioned models fail to generate the fish. MimicMotion again changes the man’s appearance by removing his beard.



A man wearing a white t-shirt is sitting while holding a fish in his hand.



Figure 22 | Example generations of our evaluated depth-conditioned models. We see high levels of saturation and distortions in Ctrl-Adapter and Control-A-Video, respectively. TF-T2V is the only model that synthesizes the fish well.

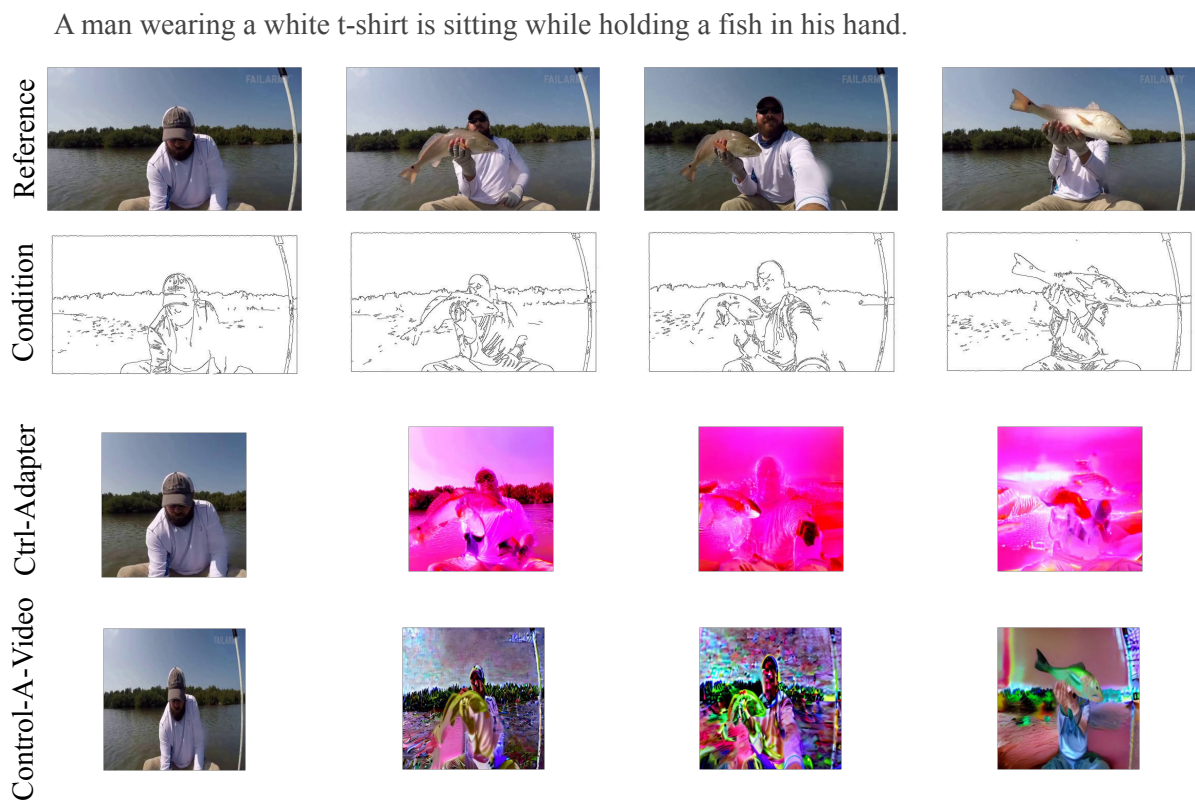


Figure 23 | Example generations of our evaluated edge-conditioned models. Ctrl-Adapter and Control-A-Video generates videos with very high levels of saturation and distortion.



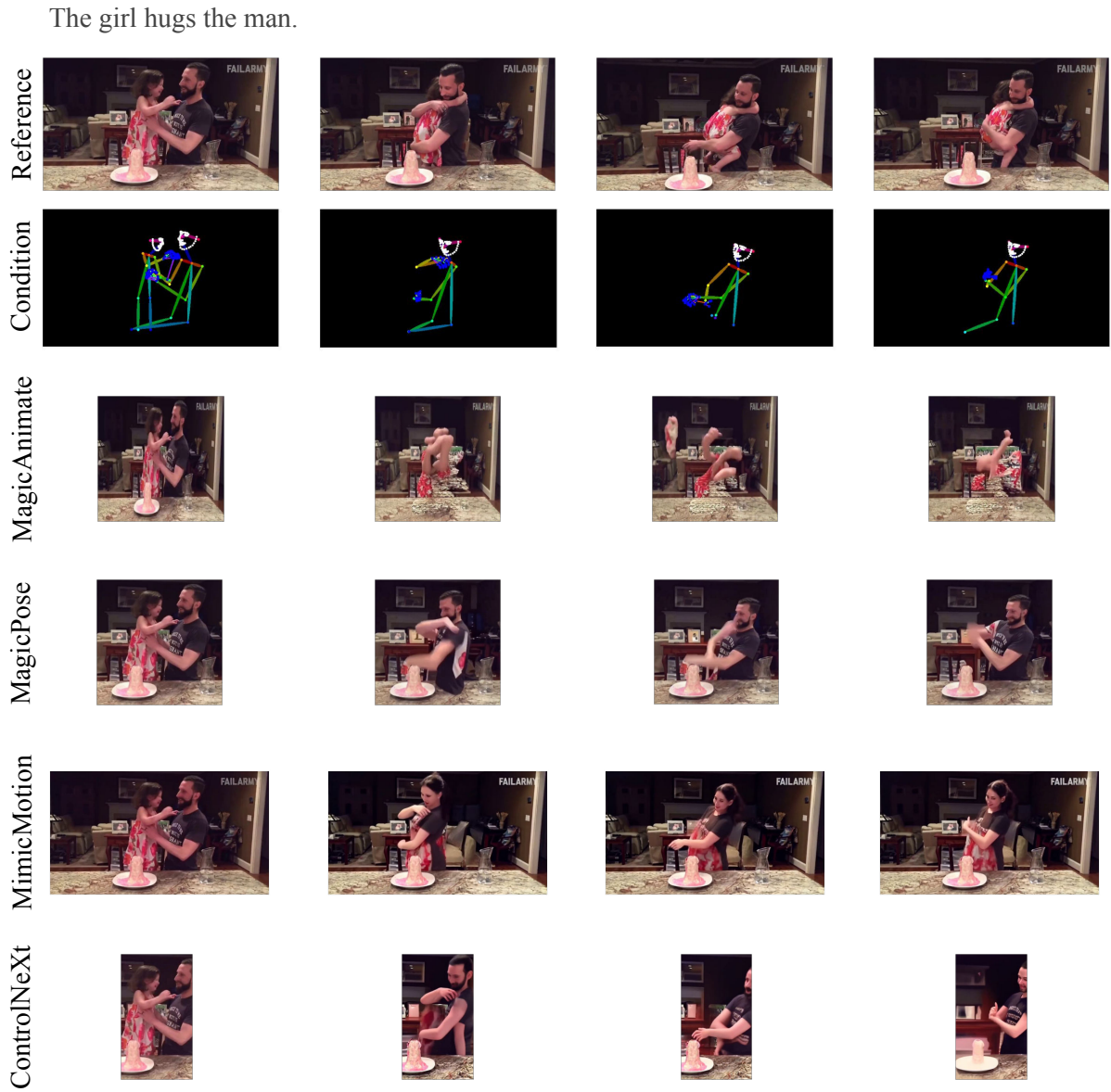


Figure 24 | Example generations of our evaluated pose-conditioned models (MagicAnimate uses dense poses). All models struggle with generating multiple humans interacting with each other consistently due to the limitations of the pose extractor. For example, MagicPose and ControlNeXt make the girl disappear, while MimicMotion merges the girl and the man into a woman.

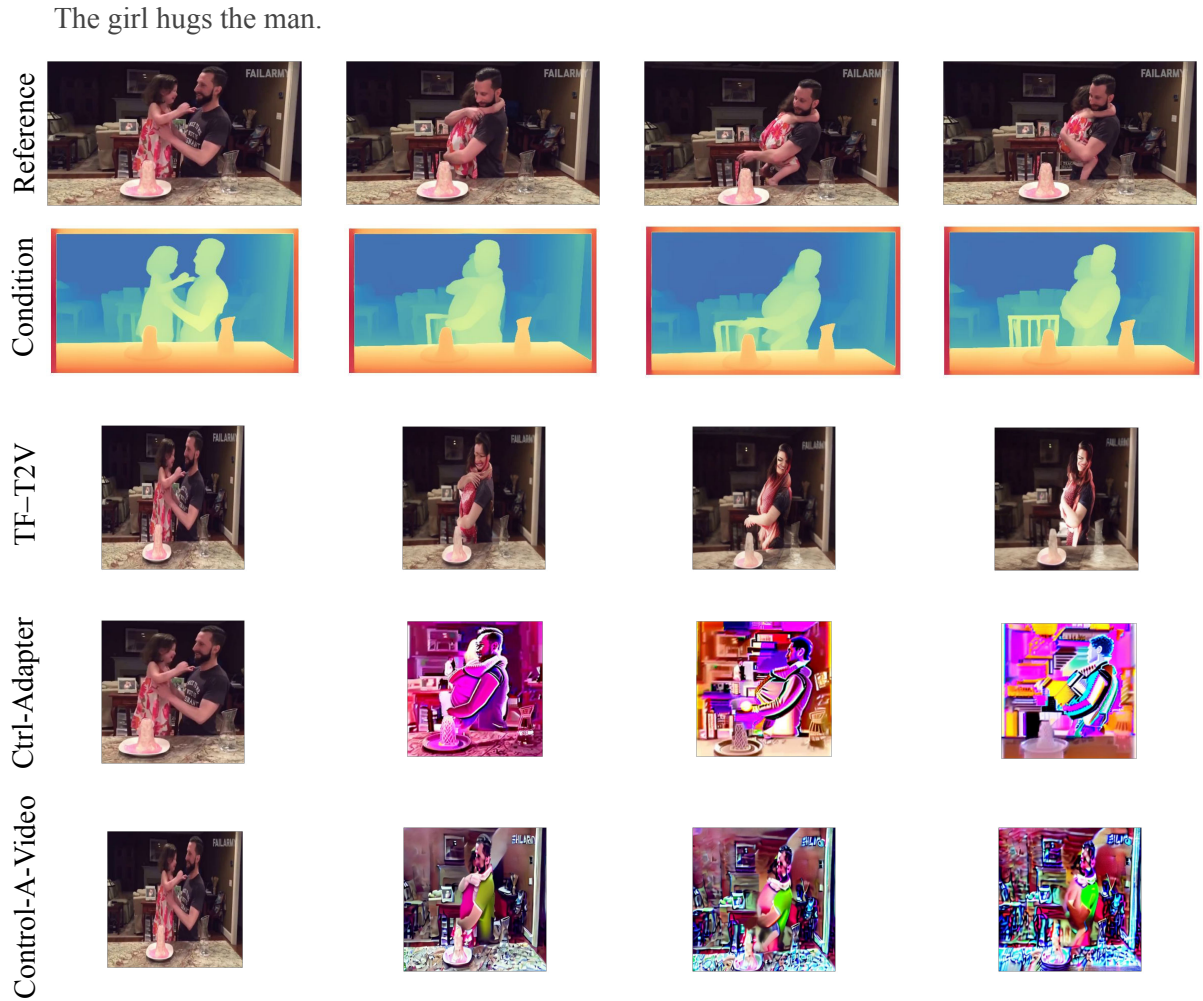


Figure 25 | Example generations of our evaluated depth-conditioned models. We can see that even TF-T2V struggles to make the two humans interact with each other, resulting in a video where the man and the girl are merged into a single person with low-quality facial traits.



Figure 26 | Example generations of our evaluated edge-based models. Once again, the generations of Ctrl-Adapter and Control-A-Video are affected by high levels of saturation and distortion, despite being a static scene.

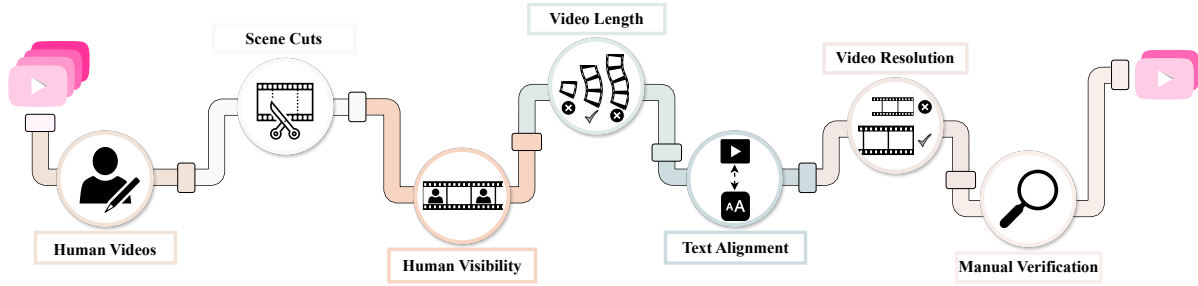


Figure 27 | **wYD data filtering pipeline.** Our pipeline includes 7 steps: identifying videos with human actors, removing scene cuts, ensuring human visibility, removing short/long videos, keeping videos with high text alignment, removing low-res videos and manual verification.

Processing step	Dev			Test		
	UVO	Oops	DiDeMo	UVO	Oops	DiDeMo
StoryBench	2332	3472	2607	3895	3726	2319
Videos of humans	2085	3009	1479	3497	3168	1356
Scene cuts	1960	2962	1497	3264	3126	1342
Human visibility	996	1800	847	1638	1938	783
Video length	941	1545	706	1550	1650	670
Text alignment	545	859	550	870	953	511
Video resolution	545	859	501	870	953	462
Manual verification (wYD)	235	323	97	346	424	119

Table 4 | Number of StoryBench entries in our datasets after each step in the wYD data preparation pipeline (see Fig. 27 and Sec. 3.1).

Baby girl one	Bikers	Daddy	Group of People Two	Lady	Mother	Persons	Tourists
A baby	Boy	Dancers	Group of children	Lady one	Musicians	Pianist	Twins
A boy	Boy	Divers	Group of men	Lady three	Officer	Player	User
A girl	Boy Four	Drummer	Group of musicians	Lady two	Old lady one	Players	Woman
A man	Boy One	Everyone	Group of people	Man	Old lady two	Police officer	Woman
A old man	Boy Three	Family	Group of people	Man	Old man	Priest	Woman
A person	Boy Two	Fighter	Group of people one	Man Five	Old woman	Rangers	Woman One
A person	Boy five	Fighters	Group of people one	Man Four	Others	Referee two	Woman Three
A woman	Boy four	Fourth man	Group of people two	Man One	Passengers	Rest	Woman Two
Baby	Boy one	Gentleman	Group two	Man One	People	Rider	Woman five
Baby	Boy one	Girl	Guitarist	Man Three	Peoples	Rider one	Woman four
Baby Boy	Boy three	Girl	Guy	Man Two	Performer	Rider one	Woman one
Baby boy	Boy two	Girl three	He	Man five	Person	Rider two	Woman one
Baby girl	Boy two	Girl One	Judge	Man four	Person	Riders	Woman three
Baby girl one	Bride	Girl Two	Kid	Man one	Person Four	Runner	Woman two
Baby girl two	Bridegroom	Girl five	Kid	Man one	Person One	Second man	Woman two
Baby girl two	Child	Girl four	Kid Four	Man one	Person Three	Singer	Women
Baby one	Child	Girl one	Kid Three	Man six	Person Two	Singers	Women
Baby two	Child one	Girl one	Kid Two	Man three	Person five	Someone	Women one
Band	Child one	Girl third	Kid four	Man three	Person four	Speaker	Young man
Batter	Child two	Girl three	Kid one	Man two	Person one	Swimmers	kid
Bichon frise	Child two	Girl two	Kid one	Man two	Person one	They	kid one
Bicyclist	Couple	Girl two	Kid three	Marchers	Person three	Third	kid three
Bicyclists	Cyclist	Girls	Kid two	Mascot	Person three	Third boy	kid two
Bike rider	Cyclist Two	Group	Kid two	Members	Person two	Third girl	person
Biker	Cyclists	Group of People One	Kids	Men	Person two	Third man	woman

Table 5 | List of unique human actors extracted from StoryBench annotations.





Figure 28 | Discarded samples due to no human actor.

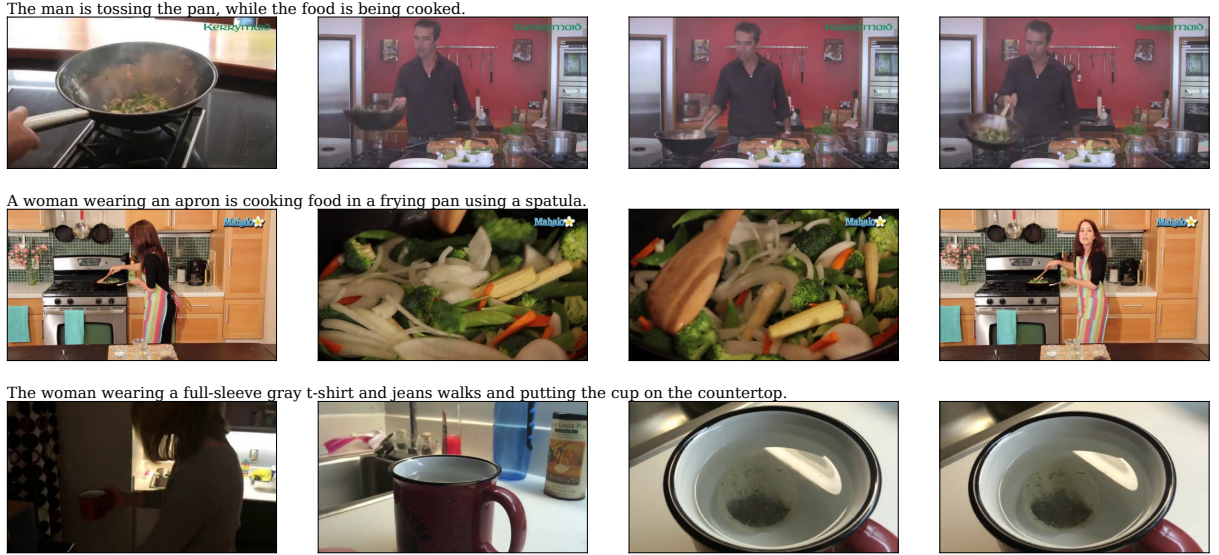


Figure 29 | Discarded samples due to scene cuts.

## B. Data annotation details

In this section, we provide additional details, statistics and samples of our data preparation and categorization processes.

**Data licenses.** We rely on three publicly available datasets to source videos for our benchmark. Kinetics [43] is released under a CC BY 4.0 license, DiDeMo [29] is released under a CC BY-NC-SA 2.0 license, and Oops [22] is released under CC BY-NC-SA 4.0 license. Moreover, we use captions and metadata collected in StoryBench [7], which are also released under a CC BY 4.0 license.

**Data filtering.** Fig. 27 shows an overview of our data filtering pipeline, while Tab. 4 details how each step of our pipeline affected the number of entries of StoryBench, and Figs. 28 to 34 show examples that were dropped at each step.

The man uses a spatula to remove the burger from the sandwich maker.



A woman wearing a brown top is folding a yellow napkin on the white table.

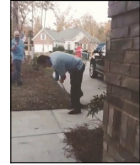
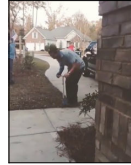
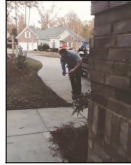
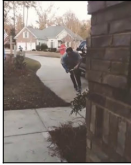


A man is sitting and reading a newspaper.



Figure 30 | Discarded samples due to low human actor’s visibility.

The man wearing a grey shirt and pants takes a turn, his scooter tire hits the corner of concrete road.



The man falls down.



A girl wearing a grey jacket is sitting at the back side inside the car and eating something while talking with the man.



Figure 31 | Discarded samples due to video duration.

Tab. 5 lists the 224 unique strings referring to human actors in our datasets. For each StoryBench caption in DiDeMo, we extract the actors using an LLM [24] with the prompt: “Which living being is performing the main action in the following caption? Reply with one word.”

Figs. 36 and 37 show the distribution of video duration and resolution for WYD, TikTok and TED-Talks. Manual video quality verification and labeling were carried through an extensive period (over two months) by the authors. Most of the resulting videos (99.5%) have a size of at least 512p. Moreover, we note that a fraction of the frames display motion blur, which is unavoidable in videos with high motion.

**Video categorization.** Fig. 38 shows our UI for video categorization, while Fig. 40 shows how different categories interact with each other.



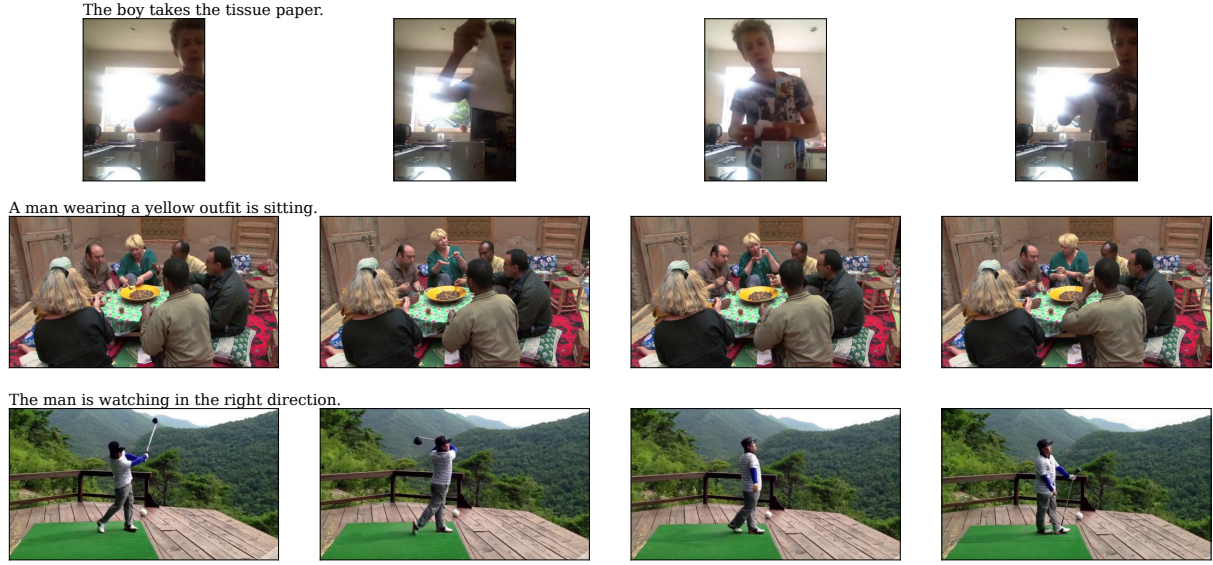


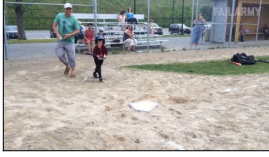
Figure 32 | Discarded samples due to low video-text alignment.



Figure 33 | Discarded samples due to low video resolution.

**Video segmentation masks.** Fig. 39 shows our UI for verifying and fixing video segmentation masks for each actor. Annotations were made at every frame using a brush to extend or delete pixels corresponding to the automatically generated segmentation masks for each human actor.

The man walks to the left while the kid is walking forward then stops and starts moving the bat.



The man accidentally hits himself.



The girl starts running after being scared from a person wearing a dinosaur costume, towards a woman a boy wearing dinosaur costume chasing the kids

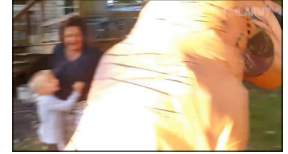


Figure 34 | Discarded samples due to manual verification.

A boy in a green t-shirt is moving forward by jumping on the inflatable playhouse than a giant ball collides with the boy.



A boy wearing a grey hoodie is skateboarding at the top of stairs.



A man wearing black-grey shorts is performing a high bar while a man wearing a black t-shirt is standing and holding a blue mattress.



A rider wearing a yellow-orange outfit is riding a bike on the soil surface while another rider is waiting on the lower end of the ramp.



A kid wearing a red-white jacket is sledding down on a snowy slope while a group of kids are moving in an upward direction.



Figure 35 | Samples from the final wYD dataset.



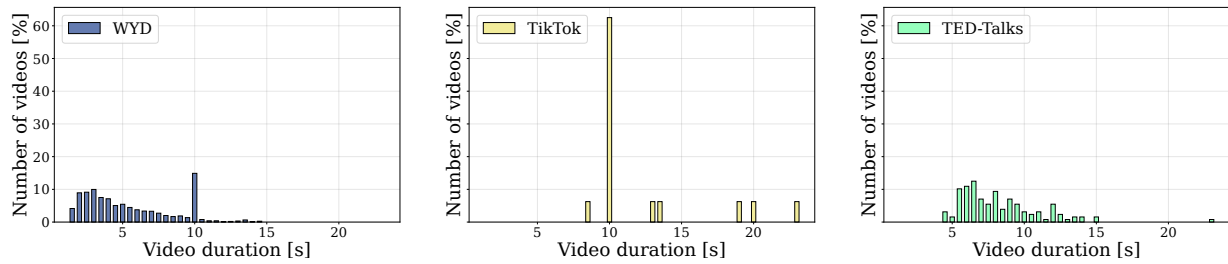


Figure 36 | Distribution of video duration in WYD, TikTok and TED-Talks. WYD covers actions lasting a few seconds and up to 15s.

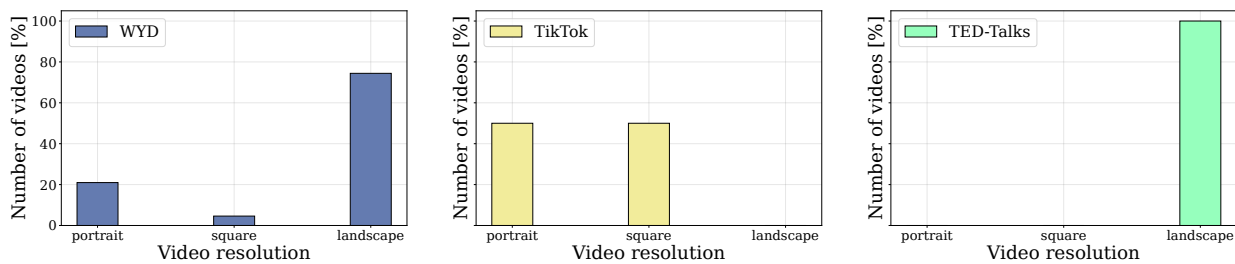


Figure 37 | Distribution of video resolution in WYD, TikTok and TED-Talks. WYD contains videos that have more diverse aspect ratios.

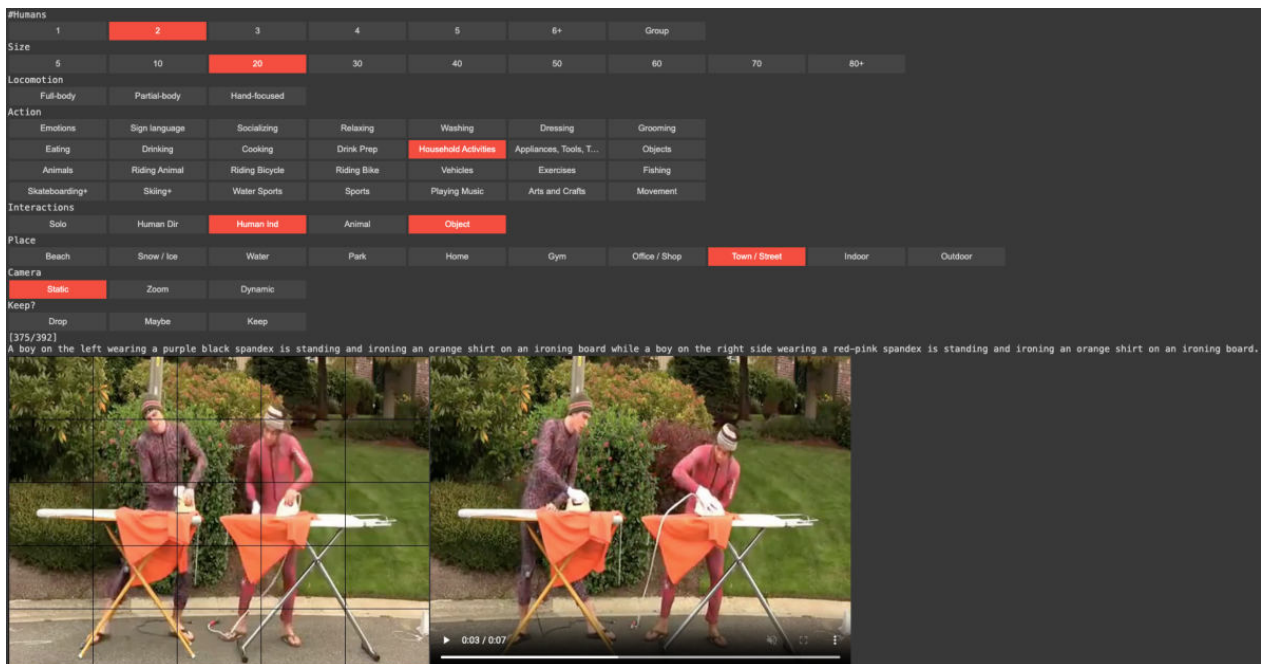


Figure 38 | UI used to manually filter and label videos in WYD according to different categories.



Figure 39 | UI used to manually fix video segmentation masks in wvd through a brush to select pixels corresponding to an actor’s mask.

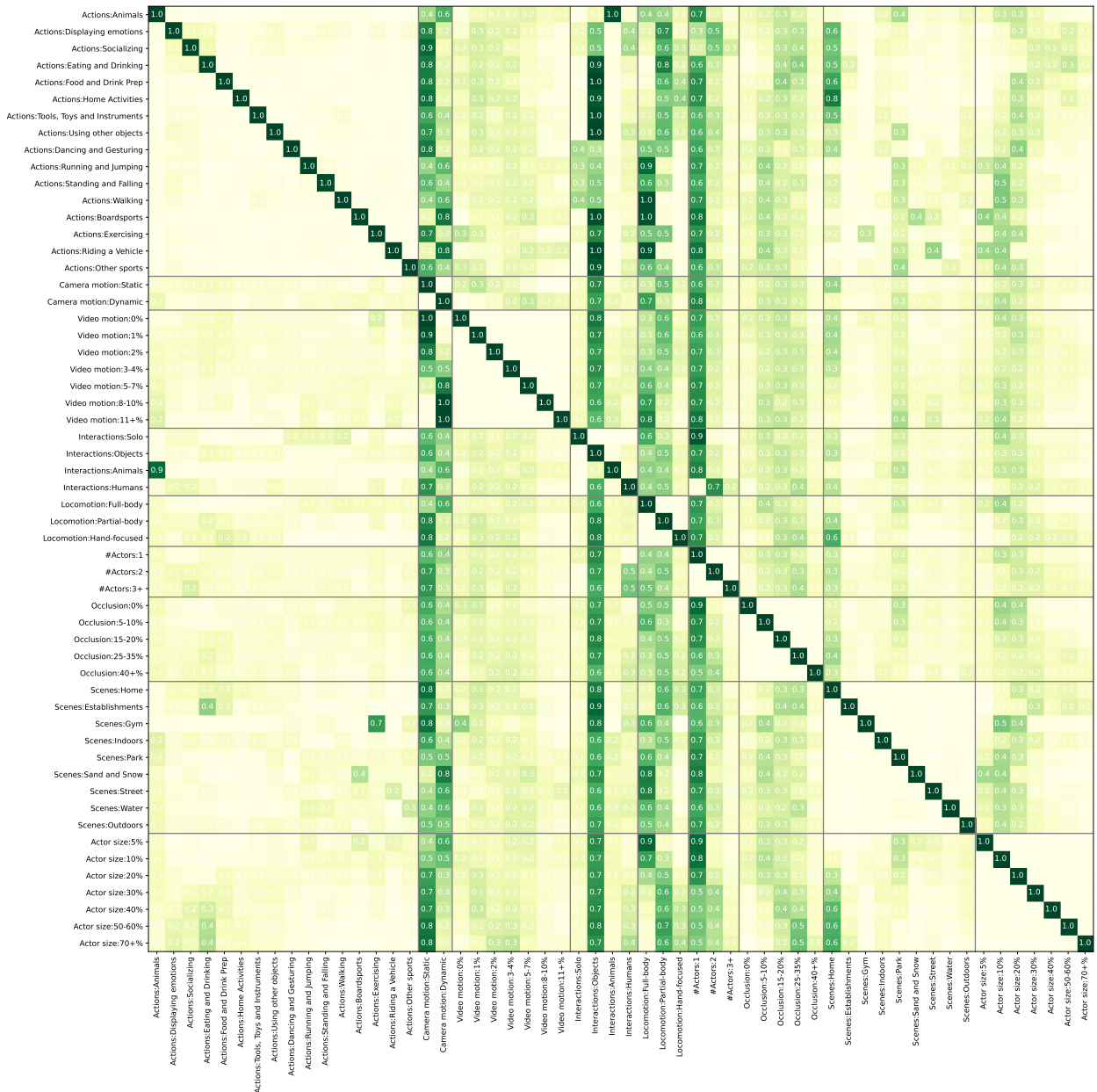


Figure 40 | **Percentage of videos overlapping between two categories.** For a given row, computes how many of its videos (in percentage) are also available in another category (column). Best viewed on a screen due to its large number of entries.

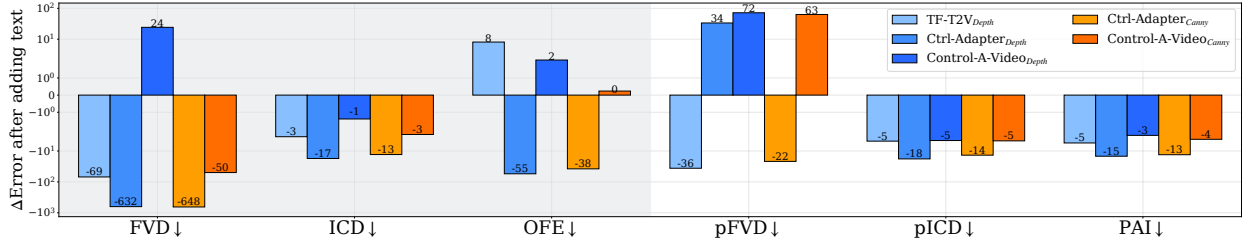


Figure 41 | **Difference in errors in wVD after adding captions to depth- and edge-conditioned models.** Adding text guidance usually improves models’ performance, except for pFVD where the Control-A-Video’s performance worsen when using either depth or edges.



Figure 42 | **Performance of best models w.r.t. ‘#Actors,’ ‘Actor size’ and ‘Actor occlusion.’** Animating multiple actors is harder than a single one. Small humans are also harder to generate precisely compared to when they cover a large portion of the frame. Performance also tends to degrade as the amount of occlusion increases.

### C. Additional results

In this section, we report complementary results from our experiments. Namely, Fig. 41 shows the difference in errors of depth- and edge-conditioned models when adding captions as an additional source of guidance. Figs. 42 to 45 report category-level performance of our best models (MimicMotion, ControlNeXt and TF-T2V) according to sample-level metrics (ICD, OFE, pICD, pAPE).



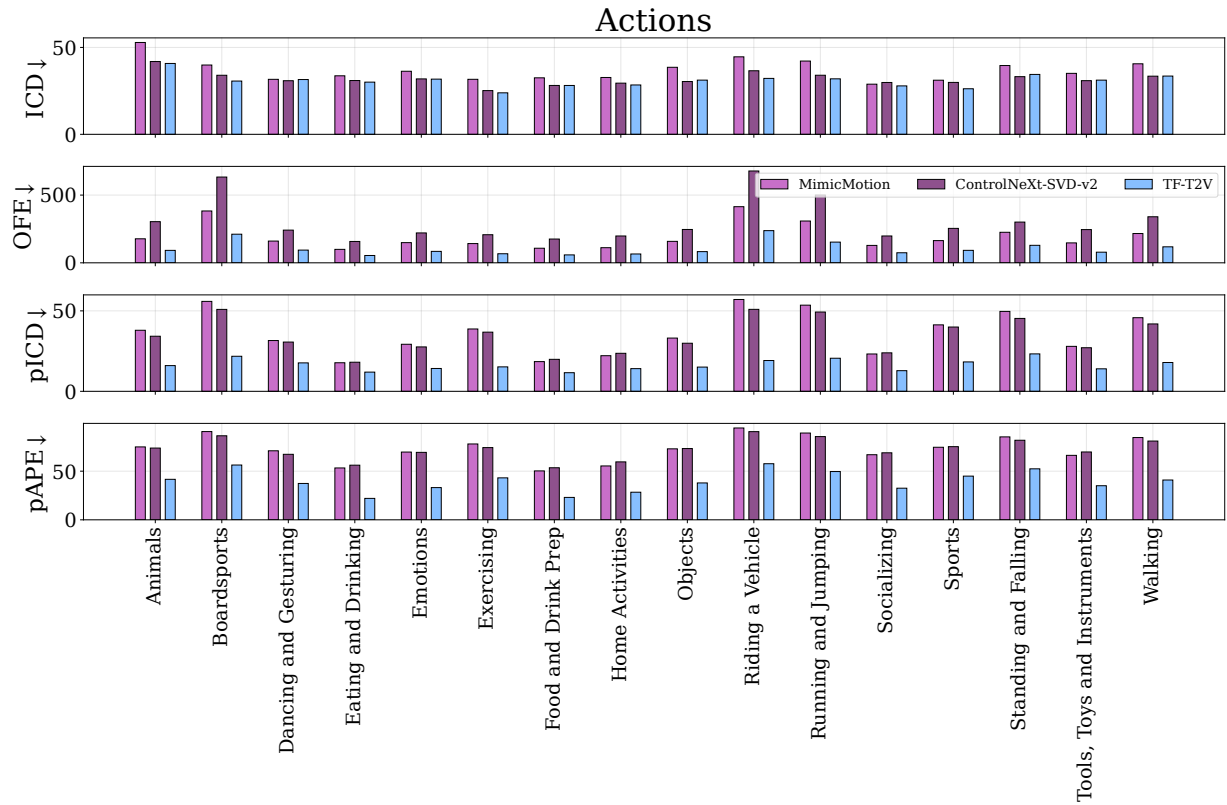


Figure 43 | **Performance of best models w.r.t. 'Actions.'** Actions involving animals, riding a vehicle, running and jumping, and boardsports are challenging for SOTA models (especially pose-conditioned ones). Atypical movements, e.g., standing up and falling down, are also hard.

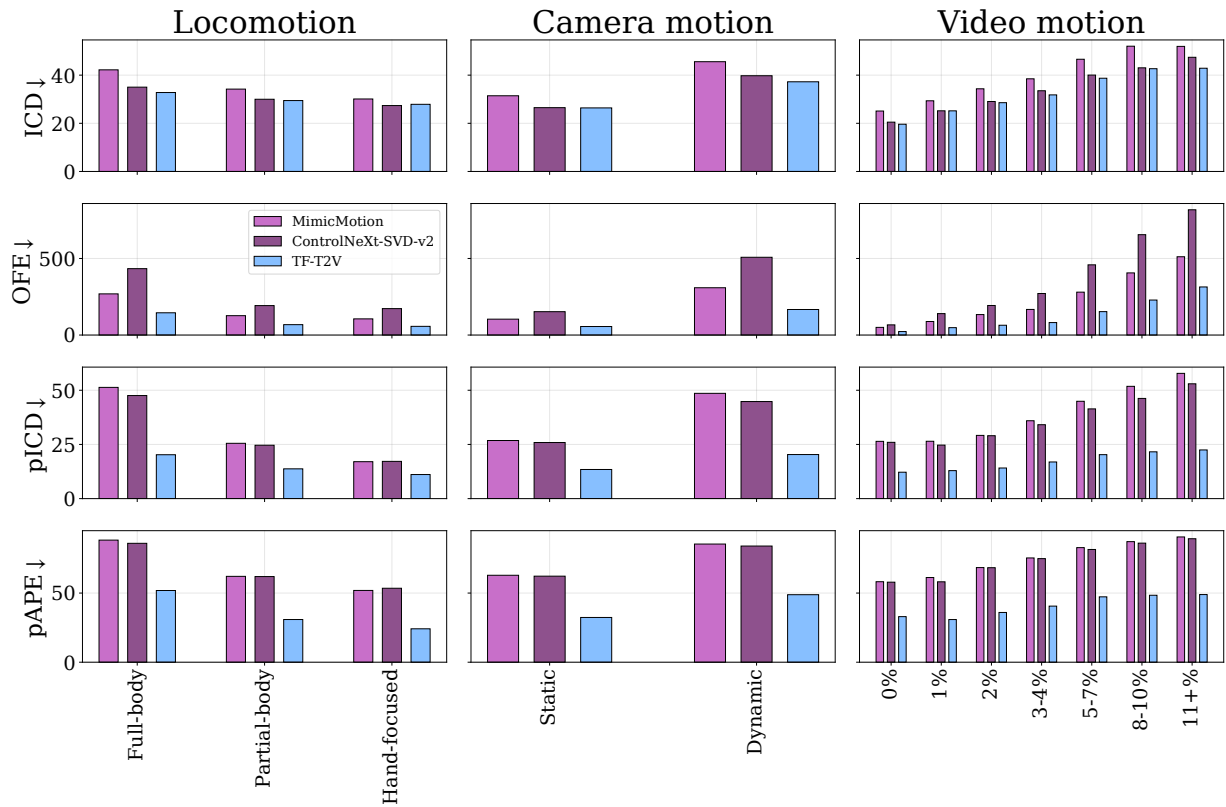


Figure 44 | **Performance of best models w.r.t. 'Locomotion,' 'Camera motion' and 'Video motion.'** Videos with full-body locomotion are more challenging to generate due to the larger changes required. Dynamic videos with high levels of motion are more challenging. Depth-conditioned TF-T2V shows smaller OFE on dynamic videos as a result of being able to rely on background depth information.

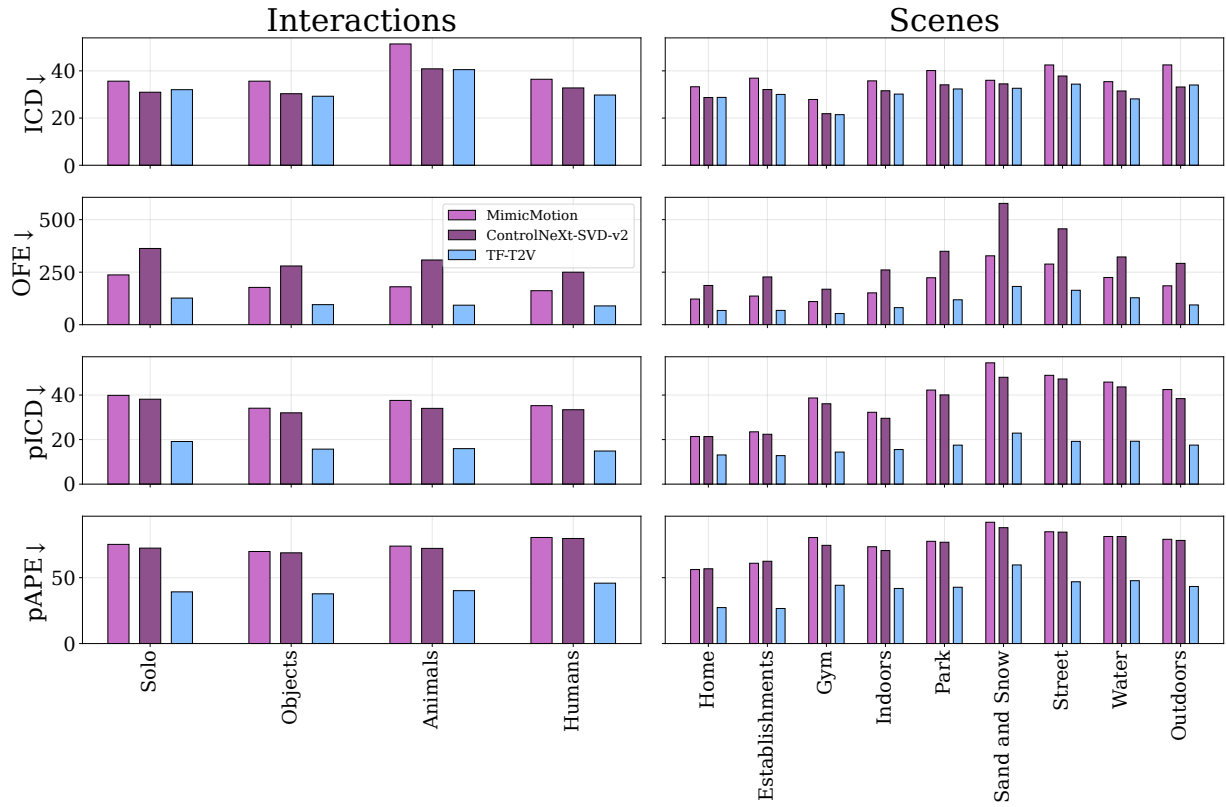


Figure 45 | **Performance of best models w.r.t. 'Interactions' and 'Scenes.'** Generating videos of humans interacting with animals or other humans is more difficult than solo videos. Outdoors scenes (e.g., on sand and snow, street, by the water) are also harder for SOTA models.

## D. Evaluations

In this section, we report the performance of our evaluated models according to several automatic metrics and detail our human evaluation protocol.

**Automatic metrics.** Figs. 46 to 49 show how additional metrics score our seven models w.r.t. overall and human video quality, frame-by-frame similarity and video motion.

We note that, when computing automatic metrics, the pre-processing operations of a given video generation model are also applied to the reference videos. This is because current models were not initially designed to support all aspect ratios, and comparing their generations with the original reference videos would result in unfair evaluations. For instance, ControlNeXt generates portrait videos only. If we had not applied the same transformations to the reference videos, we would not have been able to compute pixel-level metrics. Moreover, this ensures that the results obtained with pAPE capture scale differences (despite model-specific resolutions) and correctly identifies the re-scale and re-center issue in MimicMotion and ControlNeXt described in Sec. 6. We encourage future work to develop models that can process different aspect ratios so as to ensure fully comparable results and benchmarking on WYD.

**Side-by-side human evaluations setup.** For side-by-side evaluation, we sample 100 random videos from WYD and ask four researchers familiar with the task. Each researcher annotates 25 comparisons for each model pair and across four evaluation setups: (i) video quality, (ii) video motion similarity, (iii) human quality w.r.t. reference, and (iv) human motion w.r.t. reference.

For video quality, we compare all 21 model pairs; while we only compare five model pairs (MimicMotion vs. ControlNeXt, MagicPose vs. ControlNeXt, MagicPose vs. Ctrl-Adapter, MimicMotion vs. TF-T2V, TF-T2V vs. Control-A-Video) on the other tasks due to the increased amount of time required for careful evaluations.

An example of our UI for side-by-side evaluations is shown in Fig. 50, where we remove the actors' segmentation masks for setup (ii), and only show the generated videos for setup (i). We used the following the templates for evaluation.

1. **Video quality:** Choose the video that you think is of highest quality (less defects, distortions, artifacts, excessive blur, etc.). If both have the same quality, choose the one that is more appealing to you (more interesting, better composition, etc.). If both videos are equally appealing, click on "Equally Good/Bad."
2. **Video motion similarity:** Choose the video that you think best matches the motion of the entire reference video (shown in the middle). Please try to ignore potential defects or bad quality of the videos. If both videos equally follow the motion of the reference video, click on "Equally Good/Bad."
3. **Human quality w.r.t. reference:** Choose the video that you think has the highest quality (less defects, distortions, artifacts, excessive blur, etc.) for the people highlighted in the reference video (shown in the middle). If the highlighted people in both videos are equally good/bad, click on "Equally Good/Bad."
4. **Human motion w.r.t. reference:** Choose the video that you think best matches the movements of the people in the reference video (shown in the middle). Please try to ignore potential defects or bad quality of the videos. If both videos equally follow the motion of the reference video, click on "Equally Good/Bad."

## E. Ethics statement

The aim of *What Are You Doing?* (WYD) is to enable better evaluation of current and future controllable video generation models with respect to human characters and motion, which arguably are of particular

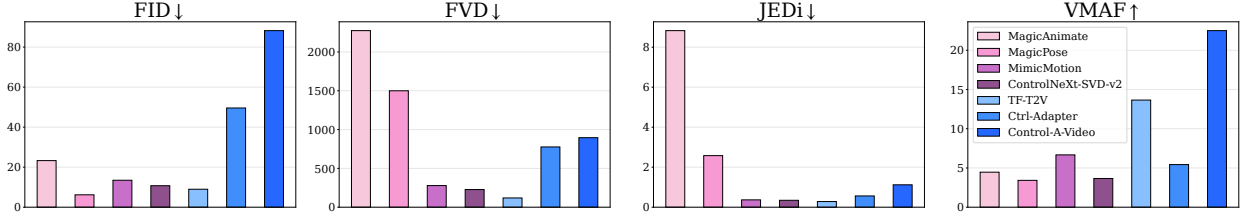


Figure 46 | **Comparison of video quality metrics on wYD.** FID favors MagicPose’s flickering videos, and VMAF ranks Control-A-Video’s videos with distortions and artifacts first. FVD and JEDI rank video generations with high agreement to human judgments.

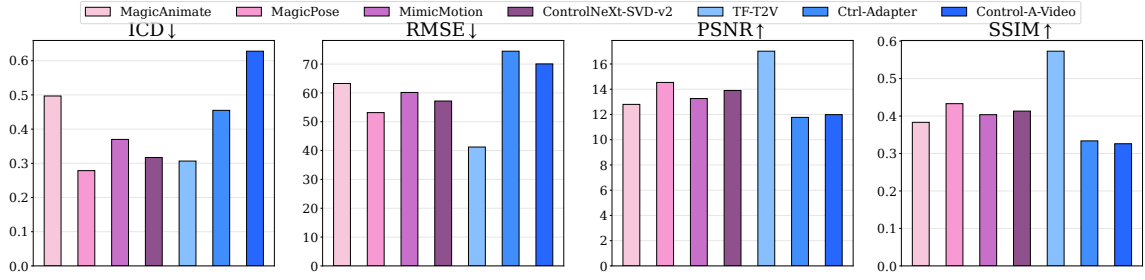


Figure 47 | **Comparison of frame-by-frame similarity metrics on wYD.** PSNR and SSIM prefer videos of distorted people from MagicAnimate more than videos from Ctrl-Adapter, unlike humans. Similarly, RMSE does not agree with human annotators who prefer videos from Ctrl-Adapter over those from Control-A-Video. ICD matches human agreement more often than other metrics.

importance to people. While this kind of models have great potential to assist and augment human creativity, there are broader societal issues that need to be considered when developing these models.

Video generative models may be misused to generate fake, hateful, explicit or harmful content. For example, they could be used to spread misinformation and portray false situations by synthesizing fake content (*i.e.*, deepfakes). To mitigate these harms, digital watermarks can be applied to generated videos [56] to identify whether a given video was produced by a particular model.

Generative models rely on massive amounts of data harvested from the Web, which reflect social stereotypes, oppressive viewpoints, and harmful associations to marginalized identity groups [4, 5, 58]. It is essential that generated content avoids perpetuating harmful stereotypes and respects cultural sensitivities. In fact, models primarily trained on samples with English data may reflect Western cultures [52, 66]. We acknowledge that our benchmark does not explicitly aim to encompass several cultures and populations, and it may perpetuate biases present in the datasets on which it is based. We encourage future work to develop training and evaluation setups that aim to widen the social and cultural representations of these technologies.

Moreover, we note that training video generative models is computationally expensive, both financially (*e.g.*, hardware and electricity) and environmentally, due to the carbon footprint of modern tensor processing hardware. We encourage future research that explores more efficient architectures.

Due to the impacts and limitations described above, we remark that wYD aims to measure progress in video generation research. By no means should our data be extended for use in sensitive domains. We believe that generative technologies, like the type of controllable image-to-video models that can be evaluated in wYD, can become useful tools to enhance human productivity and creativity.

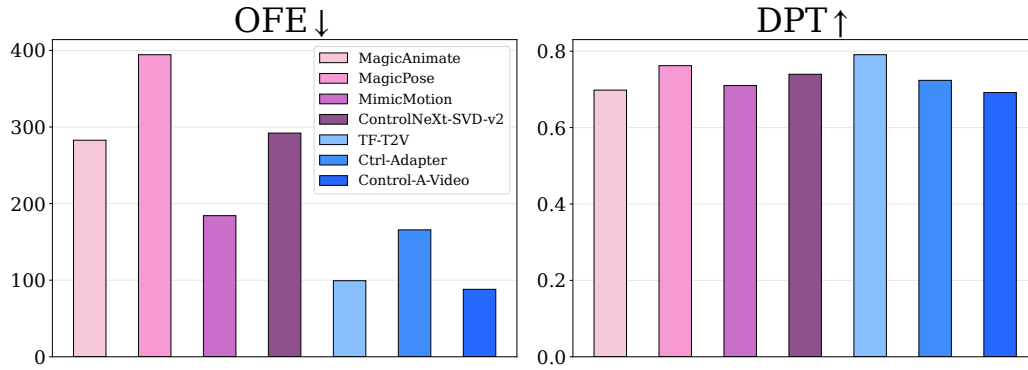


Figure 48 | **Comparison of video motion similarity metrics on wVD.** We see that a depth-based metric (DPT) ranks the flickering generations from MagicPose as the second best ones, and those of pose-guided ControlNeXt better than those of depth-conditioned Ctrl-Adapter and Control-A-Video, which better generate videos with dynamic camera. OFE better agrees with the human rankings.

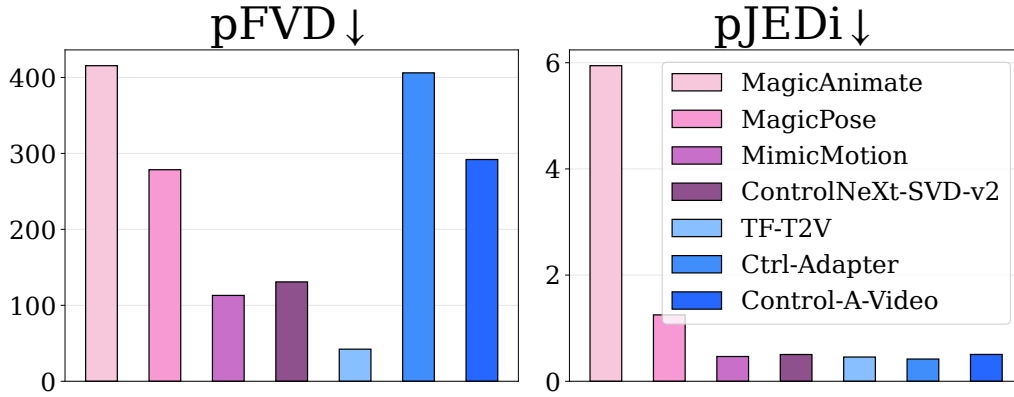


Figure 49 | **Comparison of human-level video quality metrics on wVD.** We find that pJEDI does not extract useful features when blacking out the pixels not corresponding to human video segmentation masks. For instance, it suggests that Control-A-Video generates the best people, unlike our human annotators.



Figure 50 | **UI used to collect human preferences in side-by-side evaluations for wVD.** We remove the actors' segmentation masks when comparing video motion similarity. No reference video is shown for video quality comparisons.